The Valuation of Weather Derivatives using Partial Differential Equations

Clare Harris

1 September 2003

Submitted to the Department of Mathematics, University of Reading, in partial fulfilment of the requirements for the Degree of Master of Science

Abstract

In this dissertation we derive and solve numerically a partial differential equation (PDE) for the value of a weather derivative. We use historical data to suggest a stochastic process that describes the evolution of temperature and cumulative heating degree days, and then use this process to derive a convection-diffusion PDE for the value of a heating degree day option contract. This historical data is also used, together with expectation theory, to derive a valuation result which we employ as a boundary condition for our PDE. We investigate and implement various finite difference schemes, including the semi-Lagrangian method, for solving the PDE numerically. Our numerical results are then compared with those produced by the more traditional valuation techniques of Monte Carlo simulation and Burn Analysis.

Acknowledgements

I would like to thank my supervisors, Professor M.J. Baines and Dr P. McCabe, for their help and guidance during the research for and writing of this dissertation.

I would also like to thank Andy for his support and encouragement during the year.

In addition, I gratefully acknowledge the financial support of NERC.

I confirm that this is my own work and that the use of all material from other sources has been properly and fully acknowledged.

Contents

List of Figures

List of Abbreviations

CDD	Cooling Degree Day(s)
EUR	Euro(s)
EWMA	Exponentially Weighted Moving Average
HDD	Heating Degree Day(s)
PDE	Partial Differential Equation
SDE	Stochastic Differential Equation
WMO	World Meteorological Organisation

Glossary of Notation

K	Strike
cap	Payment cap
$tick$	Tick size
t	Time from start of contract period
T	Length of contract period
τ	$T - t$
r	Risk-free interest rate
$e^{-r(T-t)}$	Discount factor applicable from time T to time t
S	Cumulative Heating Degree Days (HDD)
X	Temperature
P	Option payoff
V	Option value
$\mathbb{E}$	Expected value
dW	Standard Wiener process
μ	Drift rate
σ	Volatility
m	Mean
s	Standard deviation
$N(m, s)$	Normal distribution with mean m, standard deviation s

Chapter 1

Introduction

1.1 Background

A derivative is a financial instrument whose value depends on the value of other, more basic underlying variables. For a weather derivative, the underlying variables are measures of the weather, for example precipitation or snowfall levels, wind speed or, most commonly, temperature.

Weather derivatives are used to control the risks of naturally-arising exposures to weather. Businesses subject to weather risk, and therefore likely to benefit from weather derivatives, include energy producers and consumers, supermarket chains, the leisure industry and agricultural industries.

The first transaction in the weather derivatives market took place in the US in 1997. Many companies then decided to hedge their seasonal weather risk after experiencing a serious loss of earnings during the very severe El Niño winter of 1997-98. Since then the market for weather derivatives has expanded rapidly, largely driven by companies in the energy sector. Although the market is still in its early stages, and is currently not very active, the number of players and volume of trades continues to increase.

The most common type of weather derivative is a 'Heating Degree Day' (HDD) or 'Cooling Degree Day' (CDD) option. This contract provides the holder with a payoff at the end of the contract period (at 'expiry') dependent on the excess of the period's cumulative Degree Days (HDD or CDD) over the 'strike' (for a 'call' option), or the excess of the strike over the cumulative Degree Days (for a 'put' option). We define these Degree Days and set out the precise form of the payoff for each type of contract in the next section.

1.2 Definitions

The Heating Degree Days (HDD) on day i are defined by

$$HDD_i = \max(18 - X_i, 0),$$

where $X_i = \frac{X_i^{\max} + X_i^{\min}}{2}$ is the average temperature measured on day i in degrees Celcius, with $X_i^{\max}$ and $X_i^{\min}$ being the maximum and minimum measured temperatures

respectively on day i.

Similarly, we define the Cooling Degree Days (CDD) on day i by

$$CDD_i = \max(X_i - 18, 0).$$

Suppose we have a contract period, $0 \leq t \leq T$, consisting of N days. Then the cumulative number of HDD and CDD for that period are

$$\begin{aligned} H_N &= \sum_{i=1}^{N} HDD_i \quad \text{and} \\ C_N &= \sum_{i=1}^{N} CDD_i \quad \text{respectively.} \end{aligned}$$

If we denote the strike level by K and the 'tick size' (the monetary value paid out per degree Celcius) by $tick$, then the payoff for an uncapped HDD call or put option is

$$\begin{aligned} P_{call} &= \max(H_N - K, 0) \times tick \quad \text{or} \\ P_{put} &= \max(K - H_N, 0) \times tick \quad \text{respectively,} \end{aligned}$$

and similarly for an uncapped CDD call or put option.

We will work with a purchased HDD put option as an example. We will now use S to represent cumulative HDD, to be consistent with stock options, where the underlying share price is usually represented by S. In addition, we will introduce a 'payment cap', cap, which is included to avoid excessive payoffs on these contracts due to unusually extreme weather conditions. Our payoff is therefore

$$P(S) = \min\{\max(K - S, 0) \times tick, cap\}. \tag{1.1}$$

This is graphed in Figure 1.1.

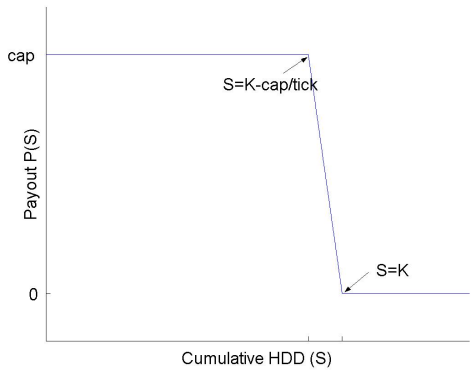

Figure 1.1: Payoff diagram for a purchased HDD put option

1.3 An Example Contract

We illustrate the previous definitions by setting out the indicative terms and conditions of a real-life HDD put option contract. The contract below was prepared by ABN Amro, but not actually traded. We shall attempt to value this example contract using various methods in later chapters.

Contract Period:	1 November 2002 up to and including 31 March 2003.
Payment Cap:	EUR 1,000,000.
Weather Unit:	On each day during the Contract Period, HDD rounded to the nearest 0.1 degrees Celcius calculated as follows: The Base Temperature for calculation of HDD is 18 degrees Celcius. If the Daily Average Temperature is below 18 degrees Celcius, HDD is equal to the Base Temperature minus the Daily Average Temperature. If the Daily Average Temperature is 18 degrees Celcius or above, HDD shall be zero.
Weather Index:	The sum of all Weather Units in the Contract Period, rounded to the nearest 0.1 degrees Celcius.
Strike Level:	1,750 Weather Units.
Weather Station:	Vlissingen (The Netherlands), WMO#:06310.
Daily Average Temperature:	The average, rounded to the nearest 0.1 degrees Celcius, of the maximum daily temperature and the minimum daily temperature, as determined by the Dutch Met Office (KNMI) at the Weather Station.
Tick Size:	EUR 5,000 per Weather Unit.
Party A Payments:	If the Weather Index in the Contract Period is greater than or equal to the Strike Level, the Party A Payment is zero. Otherwise, the Party A Payment is equal to the Tick Size multiplied by (Strike Level - Weather Index), up to a maximum of the Payment Cap.

This can be summarised by the data

$$\begin{aligned} T &= 151 \text{ (days)}, \\ K &= 1750 \text{ (}^\circ\text{C)}, \\ cap &= 1000000 \text{ (Euros)}, \\ tick &= 5000 \text{ (Euros per }^\circ\text{C)}, \end{aligned}$$

with the payoff satisfying (1.1).

1.4 Possible Valuation Methods

In order to determine a reasonable price which should be paid to acquire the weather derivative, we need to be able to value the contract at time $t = 0$ (the contract start date).

The traditional method for valuing options is via the Black-Scholes model. Unfortunately, this model is based on certain assumptions that do not apply realistically to weather derivatives, the most fundamental of these being the assumption of a tradeable underlying commodity. The underlying variables for weather derivatives, for example temperature, are not themselves tradeable in a market, and so the theory applied in the derivation of the Black-Scholes formula (see Black and Scholes [3]) is not valid.

Degree Day weather options tend therefore to be valued by developing models for either temperature or cumulative Degree Days, and then running simulations based on Monte Carlo methods or on historical data (Burn Analysis).

In this dissertation, we will develop new valuation methods based on the numerical solution of partial differential equations (PDE's) and use these to value the example contract in the previous section. We start in Chapter 2 by analysing the relevant historical temperature data, and from this, make some conclusions on the distribution of the HDD and temperature data. In Chapter 3, we use these conclusions together with expectation theory to derive a formula for our contract value. In Chapter 4, we again use the results from Chapter 2, this time to derive a partial differential equation (PDE) satisfied by the option value. Chapters 5, 6, 7 and 8 are concerned with the numerical solution of this PDE. In Chaper 9, we demonstrate the results of Monte Carlo simulations and Burn Analysis, to enable a final comparison with our previous methods.

Chapter 2

Analysis of Historical Temperature Data for the Example Contract

2.1 Introduction

Although an active or 'liquid' market does not yet exist for weather derivatives, we do have access to extensive historical weather data. This means that weather derivative models tend to be calibrated to past data. To be able to value our example contract described in section 1.3, we therefore need to analyse the relevant historical temperature data.

We have accessed the last fifty years' daily maximum and minimum temperatures for Vlissingen, The Netherlands, (the weather station of the example contract in section 1.3) from the Royal Netherlands Meteorological Institute website[1]. From this data we have calculated the daily average temperatures and Heating Degree Days (HDD) for each day in our contract period (1 November to 31 March inclusive), for each of the last fifty years.

We have then developed and tested various hypotheses about the distribution of the average temperature and HDD data, the results of which we will use in later chapters when we develop models for valuing our weather derivatives contract.

2.2 Hypotheses and Results

Hypothesis 1: *The cumulative HDD for the contract period are normally distributed.*

This hypothesis is claimed to be valid in McIntyre [11]. In our case, we have calculated the cumulative HDD for the contract period for the last fifty years, prorating the values by one day for leap years. We have then tested our hypothesis by performing a χ^2 test at the 5% level. The result of this test is that the observed distribution of

[1] www.knmi.nl

cumulative HDD is consistent with the normal distribution. We can see the closeness of fit of the observed distribution to the normal distribution from Figure 2.1.

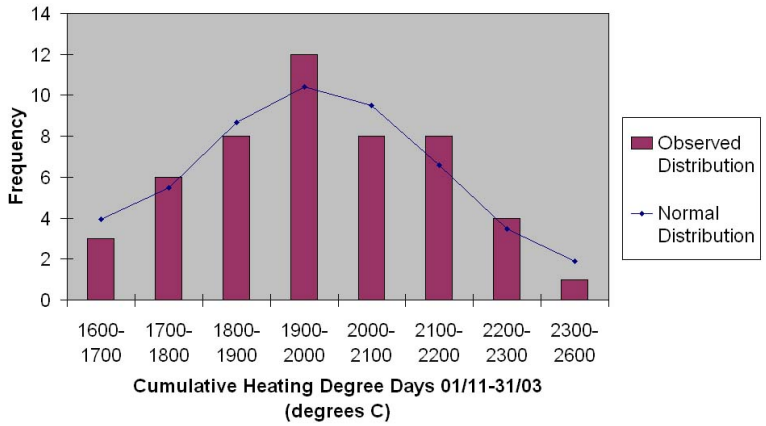

Figure 2.1: Cumulative HDD distribution for Vlissingen

We have calculated the mean (m) and standard deviation (s) of this cumulative HDD distribution for use in later chapters. We obtain

$$m = 1966.4\ (^\circ\text{C}) \quad \text{and}$$
$$s = 188.5\ (^\circ\text{C}).$$

Hypothesis 2: *The daily increments in average temperature are normally distributed.*

We have tested this hypothesis by performing Jarque-Bera tests (at the 5% level) for goodness of fit to a normal distribution, using Matlab. (This is computationally more efficient than χ^2 tests since we are performing the test for each of 151 daily increments). The results of these tests are that our hypothesis can not be rejected for 88% of the days in the contract period. Since such a high proportion of the daily increments have distributions consistent with the normal distribution, we will make the approximation that all daily increments in average temperature are normally distributed, that is, we assume that our hypothesis is true.

To use this hypothesis in valuing our example contract, we will need to know the mean and standard deviation of the average temperature increments for each day in the contract period. We deduce from the apparent random behaviour of the arithmetic mean (over the last fifty years) daily temperature increments in Figure 2.2 that a single day is too short a period for one to observe the seasonal trend in average temperature. Therefore, as is industry practice, we calculate the mean and standard deviation of each day's increment using a 30 day rolling average, exponentially weighted to give older temperature increments less weight than more recent increments. This is known as the 'Exponentially Weighted Moving Average' or EWMA (see Clewlow and Strickland [5]).

We calculate the standard deviation of the $(N+1)$th daily increment by

$$\begin{aligned} s_{N+1} &= \sqrt{\frac{1}{\sum_{i=1}^{N}\lambda^{N-i}}\sum_{i=1}^{N}\lambda^{N-i}(x_i-m)^2} \\ &\simeq \sqrt{(1-\lambda)\sum_{i=1}^{N}\lambda^{N-i}(x_i-m)^2}, \end{aligned}$$

using

$$\begin{aligned} \sum_{i=1}^{N}\lambda^{N-i} &= \sum_{i=1}^{N}\lambda^{i-1} \\ &= \frac{1-\lambda^N}{1-\lambda} \\ &\simeq \frac{1}{1-\lambda}, \end{aligned}$$

where x_i, $i = 1, 2, 3, \ldots, N$ is the arithmetic mean (based on 50 years of historical data) temperature increment of day i, m is the arithmetic mean of $x_1, x_2, \ldots, x_N$ and λ $(0 < \lambda < 1)$ is the decay factor which determines the relative weight given to older increments.

Similarly, we calculate the mean of the $(N+1)$th daily increment by

$$\begin{aligned} m_{N+1} &= \frac{1}{\sum_{i=1}^{N}\lambda^{N-i}}\sum_{i=1}^{N}\lambda^{N-i}x_i \\ &\simeq (1-\lambda)\sum_{i=1}^{N}\lambda^{N-i}x_i. \end{aligned}$$

We have taken the decay factor, λ, to be equal to 0.78. (Clewlow and Strickland [5] illustrates typical optimal decay factors for the prices of energy commodities, and these lie in the range $0.78 \leq \lambda \leq 0.98$. We would expect temperature increments to show the maximum possible seasonality, and so we require the minimum possible relative weight to be given to older days' increments, and hence the minimum possible decay factor.)

We see from Figure 2.2 that the EWMA mean does reflect seasonality, in that it is generally negative in the first half of the contract period (when the average temperature is decreasing) and generally positive in the second half of the contract period (when the average temperature is increasing).

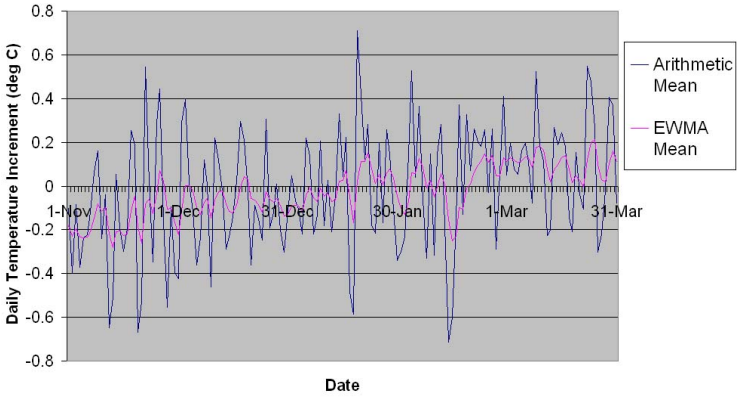

Figure 2.2: Mean daily increments in average temperature for Vlissingen

Hypothesis 3: *The daily increments in cumulative HDD are normally distributed.*

As for Hypothesis 2, we have performed Jarque-Bera tests (at the 5% level) for goodness of fit to a normal distribution, using Matlab. In this case, we find that our hypothesis can not be rejected for 78% of the days in the contract period. Although this percentage is not as high as for the temperature increment test, we still consider this to be sufficiently high a proportion that we can assume all daily increments in cumulative HDD to be normally distributed, and hence we assume that our hypothesis is true. The main reason that the daily increments in cumulative HDD do not fit a normal distribution as well as those in temperature is that the former show a long-term trend. The daily increments in cumulative HDD are just the daily HDD, which are defined by

$$HDD_i = \max(18 - X_i, 0),$$

where X_i is the average temperature of day i. For the winter contract period, we generally have $X_i \leq 18$ and so

$$HDD_i = 18 - X_i.$$

Therefore these increments show a long-term trend equal and opposite to that of the average temperature. This is illustrated for an example daily increment in Figure 2.3. We will discuss reasons for the long-term trend in average temperature in the next section.

For the calculation of the mean and standard deviation of the daily cumulative HDD increments, we note that, unlike for the daily temperature increments, the arithmetic mean (over the last fifty years) daily cumulative HDD increments do demonstrate a seasonal trend, since these increments are the daily HDD themselves. (See Figure 2.4). We see that the arithmetic mean of the daily HDD increases to the middle of the contract period (middle of winter), when the temperature is coldest, and then decreases as the temperature increases. This is consistent with the seasonality shown by the EWMA mean daily temperature increments in Figure 2.2. This implies that a single day is not too short a period for one to observe a trend in cumulative HDD, and so we can calculate our mean and standard deviation of the daily increments in the standard way.

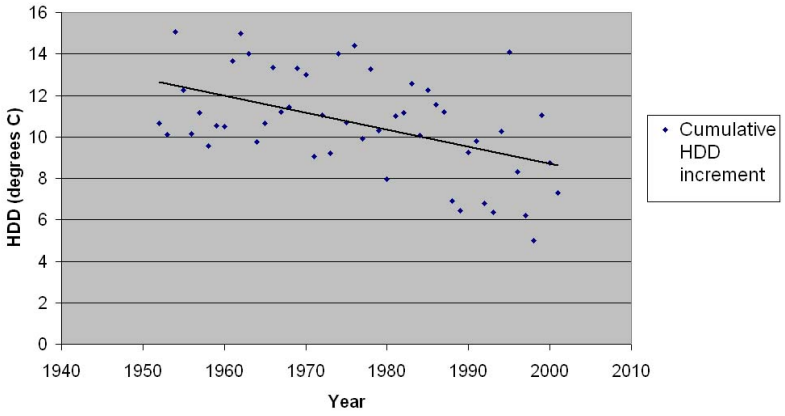

Figure 2.3: Scattergram of cumulative HDD increments for Vlissingen: 30-31 March

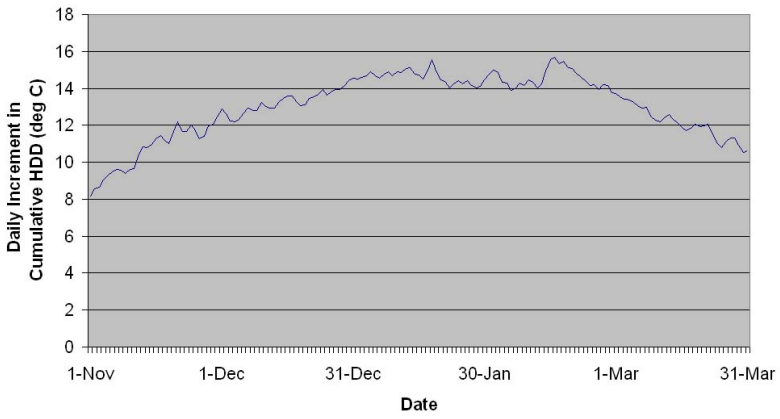

Figure 2.4: Arithmetic mean daily increments in cumulative HDD for Vlissingen

2.3 Problems with the Analysis of Historical Temperature Data

We note here some general issues with the collection and analysis of historical temperature data (see Nelken [14]), and their application to our historical data analysis:

1. Even when the data is available, there may be missing data or errors. The historical data may therefore have to be 'cleansed'. Our data source contained no gaps and no obvious anomalies, and so has not been adjusted in this respect.

2. In a leap year, the winter contract period contains an extra day. We have adjusted for this in our analysis of cumulative HDD above.

3. The weather station may have been moved due to construction, or may have been subject to other external factors (for example it may have originally been

in the sun and now be in the shade, or vice versa). This was not apparent from our data source.

4. It is not clear how many years of historical data should be considered. Dischel [6] states that fifty years is preferred (as per our analysis in the previous section), but in other cases only ten or twenty years of data are used.

5. Many cities exhibit the 'urban island effect', where, due to heavy industrial activity, the weather gradually becomes warmer in that area. The global warming effect is also apparent all over the world. We have graphed the average temperature for the contract period for the last fifty years (see Figure 2.5), and observed that an increase of almost 2 °C (from 4.1 °C to 5.9 °C) appears to have occurred. It may therefore be reasonable to linearly shift the earlier temperature data upwards by $1 - 2$ °C. Since this linear shift is very subjective, we have not attempted to alter our data in such a way, but note that this is a factor that may lead to inaccuracies in our contract valuation.

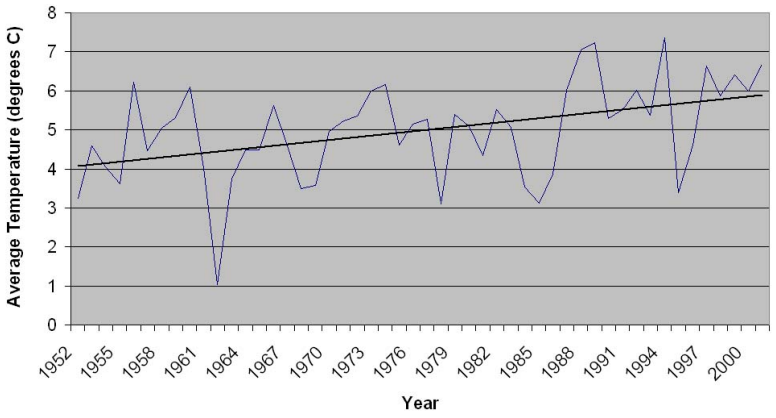

Figure 2.5: Average temperature trend for Vlissingen

6. There are extreme weather patterns that occur in some years, most notably the El Niño and La Niña, which, although directly affecting the water temperatures in the eastern and central equatorial Pacific Ocean, also have important consequences for weather and climate around the globe. Since these occur fairly frequently (El Niño approximately every two to seven years) and their impact on Europe is very difficult to quantify, we have not adjusted our historical data for these events.

Chapter 3

An Expectation-Based Formula

3.1 Introduction

In this chapter, we derive a similar result to that quoted in McIntyre [11], for the value of an HDD put option. The derivation makes the assumption, consistent with the results of the temperature analysis in the previous chapter, that the cumulative Heating Degree Days (HDD) over the life of a contract are normally distributed. The value of the option is then calculated as being the expected payoff of the option, appropriately discounted to account for the time value of money.

After proving this result, we apply the formula to the example contract in section 1.3, to obtain a value for this option at the contract start date.

3.2 Derivation of the Formula

We consider a general HDD put option, and use the notation set out on page vi. In addition, we define

S_T = the cumulative number of HDD at time $t = T$ (the end of the contract),

$P(S_T)$ = the option payoff at time $t = T$, neglecting the tick size and payment cap, that is,

$$P(S_T) = \max(K - S_T, 0), \tag{3.1}$$

and

V = the option value at time $t = 0$ (the contract start date), neglecting the tick size and payment cap.

(We will use $P^\star(S_T)$ and $V^\star$ to represent the option payoff and value when the tick size and payment cap are taken into consideration.)

We assume that S_T is a normally distributed random variable with mean m and standard deviation s, which means that S_T has probability density function

$$f(x) = \frac{1}{s\sqrt{2\pi}} e^{-\frac{(x-m)^2}{2s^2}}. \tag{3.2}$$

Then, neglecting the tick size and payment cap until later, since the value of the option is the discounted expected payoff, we have

$$\begin{aligned} V &= e^{-rT}\mathbb{E}[P(S_T)] \\ &= e^{-rT}\int_{-\infty}^{+\infty} P(x)f(x)dx \\ &= \frac{e^{-rT}}{s\sqrt{2\pi}}\int_{-\infty}^{+\infty} \max(K-x,0)e^{-\frac{(x-m)^2}{2s^2}}dx \end{aligned}$$

(substituting from (3.1) and (3.2)), where r is the continuously-compounded annualised risk-free interest rate.

Since

$$\max(K-x,0) = \begin{cases} K-x & \text{if } x \le K \\ 0 & \text{if } x > K \end{cases},$$

we can write the previous expression for V as

$$V = \frac{e^{-rT}}{s\sqrt{2\pi}}\int_{-\infty}^{K} (K-x)e^{-\frac{(x-m)^2}{2s^2}}dx. \tag{3.3}$$

If we define

$$z = \frac{x-m}{s},$$

then we have

$$\begin{aligned} x &= sz + m, \quad \text{and} \\ dx &= sdz, \end{aligned}$$

and, making a change of variable from x to z in (3.3) gives

$$\begin{aligned} V &= \frac{e^{-rT}}{s\sqrt{2\pi}}\int_{-\infty}^{\frac{K-m}{s}} (K-sz-m)e^{-\frac{z^2}{2}}sdz \\ &= \frac{e^{-rT}}{\sqrt{2\pi}}\int_{-\infty}^{\frac{K-m}{s}} (K-m)e^{-\frac{z^2}{2}}dz - \frac{e^{-rT}}{\sqrt{2\pi}}\int_{-\infty}^{\frac{K-m}{s}} sze^{-\frac{z^2}{2}}dz \\ &= e^{-rT}(K-m)\int_{-\infty}^{\frac{K-m}{s}} \frac{1}{\sqrt{2\pi}}e^{-\frac{z^2}{2}}dz \; + \; \frac{se^{-rT}}{\sqrt{2\pi}}\left[e^{-\frac{z^2}{2}}\right]_{-\infty}^{\frac{K-m}{s}} \\ &= e^{-rT}(K-m)\int_{-\infty}^{\frac{K-m}{s}} \frac{1}{\sqrt{2\pi}}e^{-\frac{z^2}{2}}dz \; + \; \frac{se^{-rT}}{\sqrt{2\pi}}e^{-\frac{(K-m)^2}{2s^2}} \\ &= e^{-rT}\left\{(K-m)N\left(\frac{K-m}{s}\right) + s^2 f(K)\right\}, \end{aligned} \tag{3.4}$$

where $N(x) = \frac{1}{\sqrt{2\pi}} \int_{-\infty}^{x} e^{-\frac{z^2}{2}} dz$ is the cumulative standard normal distribution function, and $f(x)$ is the normal probability density function defined in (3.2).

We now recall that the actual payoff of the option, including the tick size and payment cap is

$$P^\star(S_T) = \min\left\{\max(K - S_T, 0) \times tick, cap\right\},$$

and so the actual value is

$$\begin{aligned} V^\star &= e^{-rT}\mathbb{E}\left[P^\star(S_T)\right] \\ &= e^{-rT}\mathbb{E}\left[\min\left\{\max(K - S_T, 0) \times tick, cap\right\}\right] \\ &= \min\left\{e^{-rT}\mathbb{E}\left[\max(K - S_T, 0)\right] \times tick, e^{-rT} cap\right\} \\ &= \min\{V \times tick, e^{-rT} cap\}. \end{aligned}$$

We can therefore incorporate the tick size and payment cap in (3.4) to give a final value for the HDD put option at time $t = 0$:

$$V^\star = e^{-rT} \min\left\{\left((K - m)N\left(\frac{K - m}{s}\right) + s^2 f(K)\right) \times tick, cap\right\}. \qquad (3.5)$$

3.3 Valuation of the Example Contract in Section 1.3

For our example contract in section 1.3, we have

$$\begin{aligned} T &= 151 \text{ (days)}, \\ K &= 1750 \text{ (°C)}, \\ cap &= 1000000 \text{ (Euros)}, \quad \text{and} \\ tick &= 5000 \text{ (Euros per °C)}. \end{aligned}$$

Also, from our historical temperature data analysis in Chapter 2, we have

$$\begin{aligned} m &= 1966.4 \text{ (°C)}, \quad \text{and} \\ s &= 188.5 \text{ (°C)}. \end{aligned}$$

We will assume an annual risk-free interest rate of 5%.

These values mean that $\frac{K-m}{s}$ = -1.1480 (to 4 d.p.), and hence that $N\left(\frac{K-m}{s}\right) = 0.1255$ (to 4 d.p.).

Also, we can calculate $f(K) = f(1750) = 0.0011$ (to 4 d.p.).

Therefore, using formula (3.5), we obtain

$$\begin{aligned} V^\star &= e^{-0.05\times\frac{151}{365}} \min\left\{(((1750-1966.4)\times 0.1255)+(188.5^2\times 0.0011))\times 5000, 1000000\right\} \\ &= 58415. \end{aligned}$$

This shows that our expectation-based formula values the example contract in section 1.3 at 58,415 Euros at the start of the contract.

Chapter 4

A PDE for the Value of an HDD Put Option

4.1 Introduction

In this chapter, we will use Z_t to represent either the cumulative Heating Degree Days (HDD) or the temperature at time t, and derive a general PDE for the value of an HDD put option.

We will assume that Z_t satisfies the Stochastic Differential Equation (SDE)

$$dZ_t = \mu_t dt + \sigma_t dW_t, \qquad Z_0 = \widehat{Z}, \tag{4.1}$$

where μ_t is the expected drift rate at time t, σ_t is the volatility at time t of the cumulative HDD / temperature (as appropriate), and dW is a standard Wiener process.

We can make this assumption, since (4.1) is equivalent to the expression

$$Z_{t+\Delta t} - Z_t = \mu_t \Delta t + \sigma_t (W_{t+\Delta t} - W_t), \qquad Z_0 = \widehat{Z},$$

as $\Delta t \to 0$, which implies, by the definition of the standard Wiener process that

$$Z_{t+\Delta t} - Z_t \sim N(\mu_t \Delta t, \sigma_t \sqrt{\Delta t}) \tag{4.2}$$

(since $W_{t+\Delta t} - W_t \sim \epsilon\sqrt{\Delta t}$ as $\Delta t \to 0$, where $\epsilon \sim N(0,1)$). This is consistent with our data analysis in Chapter 2, which showed that it is reasonable to assume that the daily increments in both cumulative HDD and average temperature are normally distributed.

We will also assume that the value of our HDD put option at time $t = 0$ (the contract start date) is given by $V(\widehat{Z}, T)$, where T is the expiry time of the contract. We use the notation set out on page vi for the risk-free rate (r) and the strike, tick size and payment cap of the option (K, *tick* and *cap* respectively).

4.2 Derivation of the PDE

Brody *et al* [4] derived a PDE for the value of an HDD swap, where the temperature was assumed to follow a fractional Orstein-Uhlenbeck (mean-reverting) process.

Here we follow the same approach, but for an HDD put option, with the underlying cumulative HDD / temperature assumed to evolve according to the SDE (4.1). This derivation is more general than that given in Brody *et al* [4], in particular with regard to the inclusion of a generalised payoff function.

Theorem 1 *Suppose that* $\omega : \mathbb{R} \times [0,T] \to \mathbb{R}$ *is a twice continuously differentiable function with bounded derivatives, satisfying the parabolic PDE*

$$-\omega_\tau(z,\tau) - r\omega(z,\tau) + \mu_{T-\tau}\omega_z(z,\tau) + \frac{1}{2}\sigma^2_{T-\tau}\omega_{zz}(z,\tau) = 0, \tag{4.3}$$

with the initial condition

$$\omega(z,0) = P(z), \tag{4.4}$$

where $P(z)$ *is the payoff of the option. Then*

$$V(\widehat{Z},T) = \omega(\widehat{Z},T). \tag{4.5}$$

Proof First we integrate SDE (4.1) from 0 to t to give

$$Z_t = \widehat{Z} + \int_0^t \mu_s ds + \int_0^t \sigma_s dW_s. \tag{4.6}$$

We now define the process

$$\eta_t = \int_0^t \sigma_s dW_s \tag{4.7}$$

and the function

$$f(\eta,t) = \widehat{Z} + \int_0^t \mu_s ds + \eta. \tag{4.8}$$

Then (4.6),(4.7)and (4.8) imply that

$$Z_t = f(\eta_t, t). \tag{4.9}$$

Let us consider the function g of two variables, defined by

$$g(\eta,t) = e^{-rt}\omega(f(\eta,t), T-t), \tag{4.10}$$

where $f(\eta,t)$ is given by (4.8) and $\omega(z,\tau)$ is the function introduced in Theorem 1.

We first note that partial differentiation of (4.10) gives the following results:

$$\begin{aligned}
g_\eta(\eta,t) &= e^{-rt}\omega_z(f(\eta,t),T-t), && (4.11)\\
g_{\eta\eta}(\eta,t) &= e^{-rt}\omega_{zz}(f(\eta,t),T-t), \text{ and} && (4.12)\\
g_t(\eta,t) &= e^{-rt}[-r\omega(f(\eta,t),T-t) + \omega_z(f(\eta,t),T-t)\mu_t \\
&\quad -\omega_\tau(f(\eta,t),T-t)]. && (4.13)
\end{aligned}$$

Now, by applying Itô's Lemma in integral form (see equation (A.4) of Appendix A) to $g(\eta_t,t)$ when η_t follows the process (4.7), we obtain

$$g(\eta_t,t) = g(0,0) + \int_0^t \left\{ g_s(\eta_s,s) + \frac{1}{2}g_{\eta\eta}(\eta_s,s)\sigma_s^2 \right\} ds + \int_0^t g_\eta(\eta_s,s)\sigma_s dW_s.$$

At time $t = T$ this becomes

$$g(\eta_T, T) = g(0,0) + \int_0^T \left\{ g_t(\eta_t, t) + \frac{1}{2} g_{\eta\eta}(\eta_t, t)\sigma_t^2 \right\} dt + \int_0^T g_\eta(\eta_t, t)\sigma_t dW_t.$$

Substituting for g, g_η, $g_{\eta\eta}$ and g_t from (4.10),(4.11),(4.12) and (4.13) gives

$$\begin{aligned} e^{-rT}\omega(f(\eta_T, T), 0) \;=\; & \omega(f(0,0), T) + \int_0^T e^{-rt}\Big\{ -r\omega(f(\eta_t, t), T-t) \\ & + \omega_z(f(\eta_t, t), T-t)\mu_t - \omega_\tau(f(\eta_t, t), T-t)\Big\} dt \\ & + \frac{1}{2}\int_0^T e^{-rt}\omega_{zz}(f(\eta_t, t), T-t)\sigma_t^2 dt \\ & + \int_0^T e^{-rt}\omega_z(f(\eta_t, t), T-t)\sigma_t dW_t. \end{aligned}$$

From the definition of f in (4.8) and the fact that $Z_t = f(\eta_t, t)$ from (4.9), we have

$$\begin{aligned} e^{-rT}\omega(Z_T, 0) \;=\; & \omega(\widehat{Z}, T) + \int_0^T e^{-rt}\Big\{ -r\omega(Z_t, T-t) + \omega_z(Z_t, T-t)\mu_t \\ & - \omega_\tau(Z_t, T-t) + \frac{1}{2}\omega_{zz}(Z_t, T-t)\sigma_t^2\Big\} dt \\ & + \int_0^T e^{-rt}\omega_z(Z_t, T-t)\sigma_t dW_t. \end{aligned} \tag{4.14}$$

Taking expectations of both sides of (4.14), and using the fact that

$$\mathbb{E}\left[\int_0^T \phi(t) dW_t\right] = 0$$

for a Wiener process dW_t and any bounded, suitably measurable function $\phi(t)$ (see Jäckel [10]), we deduce that

$$\begin{aligned} e^{-rT}\mathbb{E}\left[\omega(Z_T, 0)\right] \;=\; & \omega(\widehat{Z}, T) + \mathbb{E}\Bigg[\int_0^T e^{-rt}\Big\{ -r\omega(Z_t, T-t) + \omega_z(Z_t, T-t)\mu_t \\ & - \omega_\tau(Z_t, T-t) + \frac{1}{2}\omega_{zz}(Z_t, T-t)\sigma_t^2\Big\} dt\Bigg]. \end{aligned} \tag{4.15}$$

Now, we know that the value of our HDD put option at time $t = 0$ must be equal to the expected value of the payoff from the option, discounted back in time, that is,

$$V(\widehat{Z}, T) = \mathbb{E}\left[e^{-rT}P(Z_T)\right]. \tag{4.16}$$

We now add (4.16) 'side by side' to (4.15), to give

$$V(\widehat{Z},T)+e^{-rT}\mathbb{E}\left[\omega(Z_T,0)\right]=\omega(\widehat{Z},T)+\mathbb{E}\Bigg[\int_0^T e^{-rt}\Big\{-r\omega(Z_t,T-t)$$

$$+\omega_z(Z_t,T-t)\mu_t-\omega_\tau(Z_t,T-t)+\frac{1}{2}\omega_{zz}(Z_t,T-t)\sigma_t^2\Big\}dt\Bigg]$$

$$+\mathbb{E}\left[e^{-rT}P(Z_T)\right].$$

Rearranging, we get

$$V(\widehat{Z},T)+e^{-rT}\mathbb{E}\left[\omega(Z_T,0)-P(Z_T)\right]$$

$$=\omega(\widehat{Z},T)+\mathbb{E}\Bigg[\int_0^T e^{-rt}\Big\{-r\omega(Z_t,T-t)$$

$$+\omega_z(Z_t,T-t)\mu_t-\omega_\tau(Z_t,T-t)+\frac{1}{2}\omega_{zz}(Z_t,T-t)\sigma_t^2\Big\}dt\Bigg]. \tag{4.17}$$

Putting $t=T-\tau$ and $Z_t=z$, (4.17) becomes

$$V(\widehat{Z},T)+e^{-rT}\mathbb{E}\left[\omega(z,0)-P(z)\right]=\omega(\widehat{Z},T)$$

$$+\mathbb{E}\Bigg[\int_0^T e^{-r(T-\tau)}\Big\{-r\omega(z,\tau)+\omega_z(z,\tau)\mu_{T-\tau}-\omega_\tau(z,\tau)+\frac{1}{2}\omega_{zz}(z,\tau)\sigma_{T-\tau}^2\Big\}d\tau\Bigg].$$

Therefore by defining $\omega(z,\tau)$ to satisfy PDE (4.3) and initial condition (4.4), we obtain the result (4.5), as required. □

4.3 Boundary Conditions

In order to solve the PDE (4.3) numerically, we require in addition to initial condition (4.4), two boundary conditions on z [1] (as the PDE is first order in τ and second order in z). Since we substituted z for Z_t, z represents cumulative HDD / temperature (as appropriate) over the life of the contract.

We will investigate these boundary conditions further in subsequent chapters, but for now we will assume that the boundary conditions take the form

$$\omega(z_1,\tau)=B_1, \tag{4.18}$$

and

$$\omega(z_2,\tau)=B_2. \tag{4.19}$$

Equation (4.5) of Theorem 1 equates ω to the option value when $\tau=T$ ($t=0$), and the initial condition (4.4) equates ω to the option payoff (i.e. option value) at time $\tau=0$ ($t=T$). Therefore, although it is not explicitly stated in Theorem 1, it appears reasonable that $\omega(z,\tau)$ may be assumed to represent the value of the option at time $t=T-\tau$, when the cumulative HDD / temperature equals z. We will therefore assume that the boundary values B_1 and B_2 represent the value of the option when the cumulative HDD / temperature equals z_1 and z_2 respectively.

[1] Note that Brody *et al* [4] did not attempt to solve their PDE numerically and therefore did not consider boundary conditions.

4.4 Transformation of the PDE and Initial/Boundary Conditions

We set out to transform our PDE into one which is more easy to solve numerically.

From equation (4.3), we have

$$\omega_\tau = \frac{1}{2}\sigma^2_{T-\tau}\omega_{zz} - r\omega + \mu_{T-\tau}\omega_z,$$

and from (4.4), (4.18) and (4.19) we have the initial and boundary conditions:

$$\begin{aligned} \omega(z,0) &= P(z), \\ \omega(z_1,\tau) &= B_1, \quad \text{and} \\ \omega(z_2,\tau) &= B_2. \end{aligned}$$

If we make the transformation

$$\omega = e^{\alpha\tau}u(z,\tau),$$

the PDE becomes

$$\alpha u + u_\tau = \frac{1}{2}\sigma^2_{T-\tau}u_{zz} - ru + \mu_{T-\tau}u_z.$$

By choosing $\alpha = -r$, we obtain

$$u_\tau = \frac{1}{2}\sigma^2_{T-\tau}u_{zz} + \mu_{T-\tau}u_z, \tag{4.20}$$

with transformed initial and boundary conditions

$$u(z,0) = P(z), \tag{4.21}$$
$$u(z_1,\tau) = e^{r\tau}B_1, \quad \text{and} \tag{4.22}$$
$$u(z_2,\tau) = e^{r\tau}B_2. \tag{4.23}$$

Our option value at time $t = 0$, $V(\widehat{Z},T)$, is then given by

$$V(\widehat{Z},T) = \omega(\widehat{Z},T) = e^{-rT}u(\widehat{Z},T). \tag{4.24}$$

Equation (4.20) is a linear parabolic PDE with time-dependent coefficients, which may also be referred to as a convection-diffusion PDE (see Morton [12]). In the next chapter, we will assess the accuracy and stability of various finite difference schemes which may be used to solve this PDE numerically. In later chapters, we will apply these numerical methods to value our example contract described in section 1.3, when z represents cumulative HDD (Chapters 6 and 7) and temperature (Chapter 8) respectively.

Chapter 5

Accuracy and Stability of Numerical Schemes

5.1 Possible Numerical Schemes

Here we set out various finite difference schemes which may be proposed to provide a numerical solution to our PDE (4.20):

$$u_\tau = \frac{1}{2}\sigma^2_{T-\tau} u_{zz} + \mu_{T-\tau} u_z.$$

We make the approximation

$$u_j^n \simeq u(z_j, \tau_n),$$

where $z_j = j\Delta z$, $\tau_n = n\Delta\tau$.

Possible schemes then include the following:

1. Explicit Central-Difference:

$$\begin{aligned}\frac{u_j^{n+1} - u_j^n}{\Delta\tau} &= \frac{1}{2}\sigma^2_{T-\tau_n}\frac{1}{(\Delta z)^2}\left(u_{j+1}^n - 2u_j^n + u_{j-1}^n\right) \\ &\quad + \mu_{T-\tau_n}\frac{1}{2\Delta z}\left(u_{j+1}^n - u_{j-1}^n\right). \end{aligned} \tag{5.1}$$

2. Implicit Central-Difference:

$$\begin{aligned}\frac{u_j^{n+1} - u_j^n}{\Delta\tau} &= \frac{1}{2}\sigma^2_{T-\tau_{n+1}}\frac{1}{(\Delta z)^2}\left(u_{j+1}^{n+1} - 2u_j^{n+1} + u_{j-1}^{n+1}\right) \\ &\quad + \mu_{T-\tau_{n+1}}\frac{1}{2\Delta z}\left(u_{j+1}^{n+1} - u_{j-1}^{n+1}\right). \end{aligned} \tag{5.2}$$

3. Crank-Nicolson:

$$\begin{aligned}\frac{u_j^{n+1}-u_j^n}{\Delta\tau} &= \frac{1}{2}\left\{\frac{1}{2}\sigma^2_{T-\tau_n}\frac{1}{(\Delta z)^2}(u_{j+1}^n-2u_j^n+u_{j-1}^n)\right.\\ &\quad\left.+\frac{1}{2}\sigma^2_{T-\tau_{n+1}}\frac{1}{(\Delta z)^2}(u_{j+1}^{n+1}-2u_j^{n+1}+u_{j-1}^{n+1})\right\}\\ &\quad+\frac{1}{2}\left\{\mu_{T-\tau_n}\frac{1}{2\Delta z}(u_{j+1}^n-u_{j-1}^n)\right.\\ &\quad\left.+\mu_{T-\tau_{n+1}}\frac{1}{2\Delta z}(u_{j+1}^{n+1}-u_{j-1}^{n+1})\right\}. \end{aligned} \tag{5.3}$$

4. Crank-Nicolson with Downwind/Upwind Convection:

$$\begin{aligned}\frac{u_j^{n+1}-u_j^n}{\Delta\tau} &= \frac{1}{2}\left\{\frac{1}{2}\sigma^2_{T-\tau_n}\frac{1}{(\Delta z)^2}(u_{j+1}^n-2u_j^n+u_{j-1}^n)\right.\\ &\quad\left.+\frac{1}{2}\sigma^2_{T-\tau_{n+1}}\frac{1}{(\Delta z)^2}(u_{j+1}^{n+1}-2u_j^{n+1}+u_{j-1}^{n+1})\right\}\\ &\quad+\begin{cases}\mu_{T-\tau_n}\frac{1}{\Delta z}\left(u_{j+1}^n-u_j^n\right) \text{ if } \mu_{T-\tau_n}>0\\ \mu_{T-\tau_n}\frac{1}{\Delta z}\left(u_j^n-u_{j-1}^n\right) \text{ if } \mu_{T-\tau_n}<0.\end{cases}\end{aligned} \tag{5.4}$$

5.2 Accuracy and Stability Results

For each of the above schemes, we have determined the scheme's accuracy by calculating the truncation error, and investigated the scheme's stability by 'freezing' the coefficients in time and then performing Fourier stability analysis. (See the following section for an example of these calculations.) The results are as follows:

Scheme	Accuracy	Fourier Stability
Explicit Central-Difference	$O(\Delta\tau)+O((\Delta z)^2)$	Stable if $\max_{\tau_n}(\sigma^2_{T-\tau_n})\Delta\tau \le (\Delta z)^2$ and $\max_{\tau_n}\lvert\mu_{T-\tau_n}\rvert\Delta\tau \le \Delta z$
Implicit Central-Difference	$O(\Delta\tau)+O((\Delta z)^2)$	Unconditionally Stable
Crank-Nicolson	$O((\Delta\tau)^2)+O((\Delta z)^2)$	Unconditionally Stable
Crank-Nicolson with Downwind/Upwind Convection	$O(\Delta\tau)+O(\Delta z)$	Stable if $\max_{\tau_n}\lvert\mu_{T-\tau_n}\rvert\Delta\tau \le \Delta z$

We can see from these results that the Crank-Nicolson scheme (5.3) has the greatest level of accuracy whilst also being unconditionally Fourier stable. This is therefore the preferred scheme out of those listed in the previous table. In the next section, we detail the accuracy and stability calculations for this chosen scheme, and in Chapter 6, we demonstrate how this scheme is implemented to approximately solve our PDE.

5.3 Accuracy and Stability Calculations for the Crank-Nicolson Scheme

5.3.1 Accuracy

We define the discrete linear operator, L_h, by

$$\begin{aligned} L_h u_j^n \equiv \frac{u_j^{n+1} - u_j^n}{\Delta\tau} \; - \; & \frac{1}{2}\left\{ \frac{1}{2}\sigma^2_{T-\tau_n}\frac{1}{(\Delta z)^2}(u_{j+1}^n - 2u_j^n + u_{j-1}^n) \right. \\ & \left. + \frac{1}{2}\sigma^2_{T-\tau_{n+1}}\frac{1}{(\Delta z)^2}(u_{j+1}^{n+1} - 2u_j^{n+1} + u_{j-1}^{n+1}) \right\} \\ & -\frac{1}{2}\left\{ \mu_{T-\tau_n}\frac{1}{2\Delta z}(u_{j+1}^n - u_{j-1}^n) \right. \\ & \left. + \mu_{T-\tau_{n+1}}\frac{1}{2\Delta z}(u_{j+1}^{n+1} - u_{j-1}^{n+1}) \right\}. \end{aligned} \tag{5.5}$$

Then the truncation error, ϵ_j^n, is defined to be

$$\begin{aligned} \epsilon_j^n &= L_h u(z_j, \tau_n) - L_h u_j^n \\ &= L_h u(z_j, \tau_n), \end{aligned} \tag{5.6}$$

since $L_h u_j^n = 0$ by definition.

Combining (5.5) and (5.6), we obtain

$$\begin{aligned} \epsilon_j^n \; = \; & \frac{1}{\Delta\tau}\left(u(j\Delta z, (n+1)\Delta\tau) - u(j\Delta z, n\Delta\tau)\right) \\ & -\frac{1}{4(\Delta z)^2}\sigma^2_{T-\tau_n}\left(u((j+1)\Delta z, n\Delta\tau) - 2u(j\Delta z, n\Delta\tau) + u((j-1)\Delta z, n\Delta\tau)\right) \\ & -\frac{1}{4(\Delta z)^2}\sigma^2_{T-\tau_n-\Delta\tau}\left(u((j+1)\Delta z, (n+1)\Delta\tau)\right. \\ & \left. -2u(j\Delta z, (n+1)\Delta\tau) + u((j-1)\Delta z, (n+1)\Delta\tau)\right) \\ & -\frac{1}{4\Delta z}\mu_{T-\tau_n}\left(u((j+1)\Delta z, n\Delta\tau) - u((j-1)\Delta z, n\Delta\tau)\right) \\ & -\frac{1}{4\Delta z}\mu_{T-\tau_n-\Delta\tau}\left(u((j+1)\Delta z, (n+1)\Delta\tau) - u((j-1)\Delta z, (n+1)\Delta\tau)\right). \end{aligned} \tag{5.7}$$

We expand (5.7) about $(j\Delta z, n\Delta\tau)$ using Taylor series, and collect coefficients of powers of Δz and $\Delta\tau$ to give

$$\begin{aligned}\epsilon_j^n \;=\; & (u_\tau - \frac{1}{2}\sigma^2_{T-\tau}u_{zz} - \mu_{T-\tau}u_z) + \frac{\Delta\tau}{2}\left(u_{\tau\tau} - \frac{1}{2}\sigma^2_{T-\tau}u_{zz\tau} + \frac{1}{2}\sigma^{2'}_{T-\tau}u_{zz} - \mu_{T-\tau}u_{z\tau}\right.\\ & \left.+\mu'_{T-\tau}u_z\right) + (\Delta\tau)^2\left(\frac{1}{6}u_{\tau\tau\tau} - \frac{1}{8}\sigma^2_{T-\tau}u_{zz\tau\tau} + \frac{1}{4}\sigma^{2'}_{T-\tau}u_{zz\tau} - \frac{1}{8}\sigma^{2''}_{T-\tau}u_{zz}\right.\\ & \left.-\frac{1}{4}\mu_{T-\tau}u_{z\tau\tau} + \frac{1}{2}\mu'_{T-\tau}u_{z\tau} - \frac{1}{4}\mu''_{T-\tau}u_z\right)\\ & +(\Delta z)^2\left(-\frac{1}{24}\sigma^2_{T-\tau}u_{zzzz} - \frac{1}{6}\mu_{T-\tau}u_{zzz}\right) + \cdots \end{aligned} \tag{5.8}$$

(using u and τ to represent $u(j\Delta z, n\Delta\tau)$ and τ_n respectively, and $\sigma^{2'}$, $\sigma^{2''}$, μ' and μ'' to represent the first and second derivatives of σ^2 and μ with respect to τ).

We note that the first bracket of expression (5.8) is zero from the definition of the PDE itself, and the second bracket is equal to the derivative of the first bracket with respect to τ, and therefore also zero.

We therefore have

$$\begin{aligned}\epsilon_j^n \;=\; & (\Delta\tau)^2\left(\frac{1}{6}u_{\tau\tau\tau} - \frac{1}{8}\sigma^2_{T-\tau}u_{zz\tau\tau} + \frac{1}{4}\sigma^{2'}_{T-\tau}u_{zz\tau} - \frac{1}{8}\sigma^{2''}_{T-\tau}u_{zz}\right.\\ & \left.-\frac{1}{4}\mu_{T-\tau}u_{z\tau\tau} + \frac{1}{2}\mu'_{T-\tau}u_{z\tau} - \frac{1}{4}\mu''_{T-\tau}u_z\right)\\ & +(\Delta z)^2\left(-\frac{1}{24}\sigma^2_{T-\tau}u_{zzzz} - \frac{1}{6}\mu_{T-\tau}u_{zzz}\right) + \cdots, \end{aligned} \tag{5.9}$$

that is, $\epsilon_j^n = O((\Delta\tau)^2) + O((\Delta z)^2)$, which implies that scheme (5.3) is second order accurate in both τ and z.

5.3.2 Stability

Since stability is a local phenomenon, we investigate the scheme with the time-dependent coefficients fixed at $\tau = \tau_0$, say. Because the coefficients only vary slowly in time, this is not an overly restrictive assumption. We set

$$\begin{aligned}\lambda \;&=\; \frac{1}{4}\sigma^2_{T-\tau_0}\frac{\Delta\tau}{(\Delta z)^2}, \quad \text{and}\\ \nu \;&=\; \frac{1}{4}\mu_{T-\tau_0}\frac{\Delta\tau}{\Delta z},\end{aligned}$$

and the scheme becomes

$$\begin{aligned}u_j^{n+1} - u_j^n \;=\; & \lambda(u_{j+1}^n - 2u_j^n + u_{j-1}^n + u_{j+1}^{n+1} - 2u_j^{n+1} + u_{j-1}^{n+1})\\ & +\nu(u_{j+1}^n - u_{j-1}^n + u_{j+1}^{n+1} - u_{j-1}^{n+1}).\end{aligned}$$

Using the Fourier method, we now let $u_j^n = a_n e^{ikj\Delta z}$, where a is a function of τ only, and substitute this into the scheme to obtain

$$\begin{aligned} a_{n+1} - a_n &= \lambda\left(a_n(e^{ik\Delta z} - 2 + e^{-ik\Delta z}) + a_{n+1}(e^{ik\Delta z} - 2 + e^{-ik\Delta z})\right) \\ &\quad +\nu\left(a_n(e^{ik\Delta z} - e^{-ik\Delta z}) + a_{n+1}(e^{ik\Delta z} - e^{-ik\Delta z})\right) \\ &= -4\lambda\left(a_n \sin^2\left(\frac{k\Delta z}{2}\right) + a_{n+1}\sin^2\left(\frac{k\Delta z}{2}\right)\right) \\ &\quad +2i\nu\left(a_n \sin\left(k\Delta z\right) + a_{n+1}\sin\left(k\Delta z\right)\right). \end{aligned}$$

We can rearrange this to give

$$a_{n+1} = G(k)a_n,$$

where

$$G(k) = \frac{1 - 4\lambda\sin^2\left(\frac{k\Delta z}{2}\right) + 2i\nu\sin\left(k\Delta z\right)}{1 + 4\lambda\sin^2\left(\frac{k\Delta z}{2}\right) - 2i\nu\sin\left(k\Delta z\right)}$$

is the amplification factor.

For Fourier stability, we require $|G(k)| \leq 1$ so that

$$\left|1 - 4\lambda\sin^2\left(\frac{k\Delta z}{2}\right) + 2i\nu\sin\left(k\Delta z\right)\right| \leq \left|1 + 4\lambda\sin^2\left(\frac{k\Delta z}{2}\right) - 2i\nu\sin\left(k\Delta z\right)\right|,$$

that is, we require

$$\begin{aligned} 1 - 8\lambda\sin^2\left(\frac{k\Delta z}{2}\right) + 16\lambda^2\sin^4\left(\frac{k\Delta z}{2}\right) + 4\nu^2\sin^2\left(k\Delta z\right) \leq \\ 1 + 8\lambda\sin^2\left(\frac{k\Delta z}{2}\right) + 16\lambda^2\sin^4\left(\frac{k\Delta z}{2}\right) + 4\nu^2\sin^2\left(k\Delta z\right), \end{aligned}$$

which is clearly satisfied for all λ, ν and k since

$$16\lambda\sin^2\left(\frac{k\Delta z}{2}\right) \geq 0.$$

Therefore the Crank-Nicolson scheme (5.3) is unconditionally Fourier stable.

Chapter 6

Solution of the PDE for Cumulative HDD

6.1 Introduction

We consider the general PDE set out in equation (4.20) of Chapter 4, and now assume that the independent variable z represents cumulative HDD. We therefore replace z by S, to be consistent with our previous notation, and the PDE (4.20) becomes

$$u_\tau = \frac{1}{2}\sigma^2_{T-\tau} u_{SS} + \mu_{T-\tau} u_S, \tag{6.1}$$

with initial and boundary conditions

$$\begin{aligned} u(S,0) &= P(S), && (6.2)\\ u(S_1,\tau) &= e^{r\tau} B_1, \quad \text{and} && (6.3)\\ u(S_2,\tau) &= e^{r\tau} B_2. && (6.4) \end{aligned}$$

(Here $P(S)$ is the option payoff, and B_1, B_2 will be taken to be the option value at $S = S_1$, $S = S_2$ respectively.)

By the definition of the option, we have

$$P(S) = \min\left\{\max(K - S, 0) \times tick, cap\right\}$$

(see equation (1.1)), which completes our initial condition.

Since HDD are positive (by definition), we know that $S \geq 0$ at all points in time. Also since S is cumulative, if $S \geq K$ at any time during the contract, we will have $S \geq K$ at expiry, and hence a zero payoff. This means that we are only required to solve for u in the region $0 \leq S \leq K$.

We therefore have

$$\begin{aligned} S_1 &= 0,\\ S_2 &= K, \quad B_2 = 0. \end{aligned}$$

The value of B_1 is less obvious. If $S = 0$ at time $t = T - \tau$, this simply tells us that the temperature has been greater than or equal to 18 °C (no HDD have occurred) up to time t. The option payoff is greater for smaller values of S at expiry. This implies that if $S = 0$ at $t = t_2$, the value of the option would be expected to be greater than if $S = 0$ at $t = t_1$, $0 \leq t_1 < t_2 \leq T$ (since if $S = 0$ later in the contract period, the value to which S accumulates by the expiry date would be expected to be lower, and hence the payoff higher, than if $S = 0$ earlier in the contract period). The boundary value B_1 is therefore an increasing function of time t, or a decreasing function of $\tau = T - t$.

To determine this function $B_1(\tau)$, we will return to the expectation approach examined in Chapter 3, and apply formula (3.5). Recall that we defined S_T to be the cumulative number of HDD at the end of the contract, and that we assumed S_T to be normally distributed with mean m and standard deviation s. Now, if $S = 0$ at a time $t = T - \tau$ from the start of the contract, S_T will accumulate over a time period of length $\tau = T - t$, rather than a period of length T. We therefore assume that the mean and standard deviation of S_T will be reduced linearly from m and s to $\frac{\tau}{T}m$ and $\frac{\tau}{T}s$ respectively in formula (3.5). The discount factor e^{-rT} will become $e^{-r\tau}$, since we are now only discounting back to the time $t = T - \tau$ rather than to the time $t = 0$.

Hence we obtain the expression

$$B_1(\tau) = e^{-r\tau} \min\left\{\left((K - \frac{\tau}{T}m)N\left(\frac{K - \frac{\tau}{T}m}{\frac{\tau}{T}s}\right) + \frac{\tau^2}{T^2}s^2 f(K)\right) \times tick, cap\right\}.$$

Using these expressions and values for $P(S)$, S_1, S_2, B_1 and B_2, our initial and boundary conditions in equations (6.2), (6.3) and (6.4) become

$$\begin{aligned} u(S,0) &= \min\left\{\max(K - S, 0) \times tick, cap\right\}, && (6.5)\\ u(0,\tau) &= \min\left\{\left((K - \frac{\tau}{T}m)N\left(\frac{K - \frac{\tau}{T}m}{\frac{\tau}{T}s}\right) + \frac{\tau^2}{T^2}s^2 f(K)\right) \times tick, cap\right\}, && (6.6)\\ u(K,\tau) &= 0, && (6.7) \end{aligned}$$

for $0 \leq S \leq K$, $0 \leq \tau \leq T$.

From equation (4.24) of Chapter 4, our option value at time $t = 0$, $V(\widehat{S}, T)$, is given by

$$V(\widehat{S}, T) = e^{-rT}u(\widehat{S}, T),$$

where $\widehat{S} = S_0$. Since S is cumulative, $S_0 = 0$, and therefore our option value at time $t = 0$ is

$$V(\widehat{S}, T) = e^{-rT}u(0, T).$$

This means that the result produced by the PDE for the option value at time $t = 0$ is determined by the boundary condition $u(0, \tau)$, and will therefore be exactly equal to that given by the expectation formula (3.5).

However, as described in section 4.3, it appears reasonable that $\omega(S, \tau) = e^{-r\tau}u(S, \tau)$

may be assumed to represent the value of the option at time $t = T - \tau$, when the cumulative HDD equals S. Therefore by solving the PDE for $u(S, \tau)$ in the region $0 \leq S \leq K$, $0 \leq \tau \leq T$, we hope to gain information about the evolution of the option value during the contract period, rather than achieving a value for the option at time $t = 0$ only.

This is beneficial since in reality weather derivatives such as our HDD put option tend to be traded during the contract period, and hence may need to be valued at any time t, $0 \leq t \leq T$. Mid-contract valuation is also necessary for a company to establish the value of its option portfolio at a point in time.

6.2 Numerical Solution

We will show how we implement the Crank-Nicolson scheme analysed in Chapter 5 to solve PDE (6.1) with initial and boundary conditions (6.5), (6.6) and (6.7).

The scheme is

$$\begin{aligned}\frac{u_j^{n+1} - u_j^n}{\Delta\tau} = \frac{1}{2}\Bigg\{ & \frac{1}{2}\sigma^2_{T-\tau_n}\frac{1}{(\Delta S)^2}(u_{j+1}^n - 2u_j^n + u_{j-1}^n) \\ & + \frac{1}{2}\sigma^2_{T-\tau_{n+1}}\frac{1}{(\Delta S)^2}(u_{j+1}^{n+1} - 2u_j^{n+1} + u_{j-1}^{n+1})\Bigg\} \\ & + \frac{1}{2}\Bigg\{\mu_{T-\tau_n}\frac{1}{2\Delta S}(u_{j+1}^n - u_{j-1}^n) \\ & + \mu_{T-\tau_{n+1}}\frac{1}{2\Delta S}(u_{j+1}^{n+1} - u_{j-1}^{n+1})\Bigg\},\end{aligned}$$

where $u_j^n \simeq u(S_j, \tau_n)$, $S_j = j\Delta S$, $\tau_n = n\Delta\tau$.

If we set

$$\begin{aligned}\lambda_n &= \frac{1}{4}\sigma^2_{T-\tau_n}\frac{\Delta\tau}{(\Delta S)^2}, \quad \text{and} \\ \nu_n &= \frac{1}{4}\mu_{T-\tau_n}\frac{\Delta\tau}{\Delta S},\end{aligned}$$

the scheme becomes

$$\begin{aligned}u_j^{n+1} - u_j^n = {} & \lambda_n(u_{j+1}^n - 2u_j^n + u_{j-1}^n) + \lambda_{n+1}(u_{j+1}^{n+1} - 2u_j^{n+1} + u_{j-1}^{n+1}) \\ & + \nu_n(u_{j+1}^n - u_{j-1}^n) + \nu_{n+1}(u_{j+1}^{n+1} - u_{j-1}^{n+1}).\end{aligned}$$

This rearranges to

$$\begin{aligned}&(-\lambda_{n+1} - \nu_{n+1})u_{j+1}^{n+1} + (1 + 2\lambda_{n+1})u_j^{n+1} + (-\lambda_{n+1} + \nu_{n+1})u_{j-1}^{n+1} \\ &= (\lambda_n + \nu_n)u_{j+1}^n + (1 - 2\lambda_n)u_j^n + (\lambda_n - \nu_n)u_{j-1}^n.\end{aligned}$$

We let j run from 0 to J, where $J\Delta S = K$. Then we can write the problem as the $(J-1)$-dimensional tridiagonal matrix system

$$\mathbf{A}\mathbf{u}^{n+1} = \mathbf{B}\mathbf{u}^n + \mathbf{c}^n,$$

where

$$\mathbf{A} = \begin{pmatrix} 1+2\lambda_{n+1} & -\lambda_{n+1}-\nu_{n+1} & 0 & \dots & 0 \\ -\lambda_{n+1}+\nu_{n+1} & 1+2\lambda_{n+1} & -\lambda_{n+1}-\nu_{n+1} & & \vdots \\ 0 & -\lambda_{n+1}+\nu_{n+1} & \ddots & \ddots & 0 \\ \vdots & & \ddots & \ddots & -\lambda_{n+1}-\nu_{n+1} \\ 0 & 0 & & -\lambda_{n+1}+\nu_{n+1} & 1+2\lambda_{n+1} \end{pmatrix},$$

$$\mathbf{B} = \begin{pmatrix} 1-2\lambda_n & \lambda_n+\nu_n & 0 & \dots & 0 \\ \lambda_n-\nu_n & 1-2\lambda_n & \lambda_n+\nu_n & & \vdots \\ 0 & \lambda_n-\nu_n & \ddots & \ddots & 0 \\ \vdots & & \ddots & \ddots & \lambda_n+\nu_n \\ 0 & 0 & & \lambda_n-\nu_n & 1-2\lambda_n \end{pmatrix},$$

and the column vectors $\mathbf{u}^n, \mathbf{u}^{n+1}$and $\mathbf{c}^n$ are given by

$$\mathbf{u}^n = \begin{pmatrix} u_1^n \\ u_2^n \\ \vdots \\ \vdots \\ u_{J-1}^n \end{pmatrix}, \mathbf{u}^{n+1} = \begin{pmatrix} u_1^{n+1} \\ u_2^{n+1} \\ \vdots \\ \vdots \\ u_{J-1}^{n+1} \end{pmatrix}, \mathbf{c}^n = \begin{pmatrix} (\lambda_{n+1}-\nu_{n+1})u_0^{n+1} + (\lambda_n-\nu_n)u_0^n \\ 0 \\ \vdots \\ 0 \\ (\lambda_{n+1}+\nu_{n+1})u_J^{n+1} + (\lambda_n+\nu_n)u_J^n \end{pmatrix}.$$

Given $\mathbf{u}^n$, we use the boundary conditions (6.6) and (6.7) to compute $\mathbf{c}^n$ and hence the right hand side of the system, $\mathbf{d}^n = \mathbf{B}\mathbf{u}^n + \mathbf{c}^n$. We then solve the system $\mathbf{A}\mathbf{u}^{n+1} = \mathbf{d}^n$ using an LU tridiagonal matrix solver. We start with $\mathbf{u}^0$, as given by the initial condition (6.5), and step forward in increments of $\Delta\tau$, until we reach $\mathbf{u}^N$, where $T = N\Delta\tau$.

Note that, if $\lambda_{n+1} \geq |\nu_{n+1}|$, then

$$\begin{aligned} -\lambda_{n+1}+\nu_{n+1} &\leq 0, \text{ and} \\ -\lambda_{n+1}-\nu_{n+1} &\leq 0, \end{aligned}$$

so

$$|-\lambda_{n+1}+\nu_{n+1}| + |-\lambda_{n+1}-\nu_{n+1}| = 2\lambda_{n+1} < |1+2\lambda_{n+1}|,$$

and therefore the matrix $\mathbf{A}$ is strictly diagonally dominant and hence non-singular, implying that the system has a unique solution.

The condition $\lambda_{n+1} \geq |\nu_{n+1}|$ is equivalent to

$$\frac{1}{4}\sigma^2_{T-\tau_{n+1}}\frac{\Delta\tau}{(\Delta S)^2} \geq \frac{1}{4}|\mu_{T-\tau_{n+1}}|\frac{\Delta\tau}{\Delta S},$$

or

$$\Delta S \leq \frac{\sigma^2_{T-\tau_{n+1}}}{|\mu_{T-\tau_{n+1}}|}, \tag{6.8}$$

for each value of n, $0 \leq n \leq N-1$. This is a sufficient condition for the system to have a unique solution.

In fact it can be shown using eigenstructure analysis that the matrix $\mathbf{A}$ is non-singular for all real values of λ_n and ν_n (see Nichols [15]) and hence that the system will always have a unique solution.

6.3 Results

We have applied the previous methodology to solve the PDE (6.1) with initial and boundary conditions (6.5), (6.6) and (6.7) for the example contract detailed in section 1.3. We used an HDD step-length of $\Delta S = 17.5$ (100 HDD steps, since we have $0 \leq S \leq 1750$), and a time-step of 1 day (151 time-steps, since $T = 151$ days).

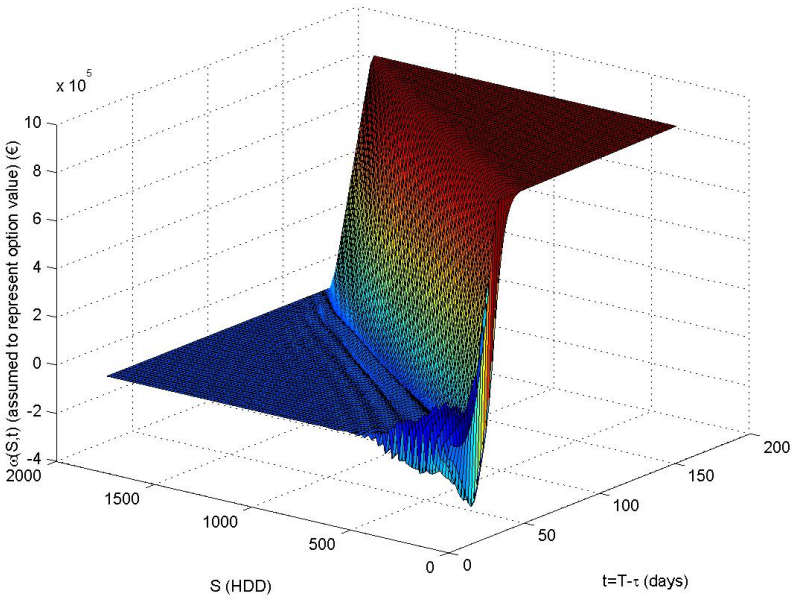

Figure 6.1: Numerical solution of PDE for Cumulative HDD using the Crank-Nicolson method

Two numerical issues are apparent from Figure 6.1:

1. It can be seen that our numerical solution contains 'spurious oscillations'. This is consistent with Morton [12], which shows that discretising the convection term using central differences for PDE's with low diffusion relative to convection can produce solutions containing spurious oscillations.

   In the case of our PDE:

   $$u_\tau = \frac{1}{2}\sigma_{T-\tau}^2 u_{SS} + \mu_{T-\tau} u_S,$$

   the diffusion term has magnitude $\frac{1}{2}\sigma_{T-\tau}^2$ and the convection term has magnitude $\mu_{T-\tau}$.

   In solving this PDE numerically we have calculated the volatility and drift of the cumulative HDD, $\sigma_{T-\tau}$ and $\mu_{T-\tau}$ respectively, using the approximation of equation (4.2):

   $$S_{t+\Delta t} - S_t \sim N(\mu_t \Delta t, \sigma_t \sqrt{\Delta t}), \tag{6.9}$$

   combined with our analysis of historical daily cumulative HDD increments in Chapter 2.

   For $\Delta t = 1$ day, equation (6.9) becomes

   $$S_{t+1} - S_t \sim N(\mu_t, \sigma_t).$$

   This tells us that

   $\mu_t = \mu_{T-\tau}$ = the mean of the daily increment $S_{t+1} - S_t$, and
   $\sigma_t = \sigma_{T-\tau}$ = the standard deviation of the daily increment $S_{t+1} - S_t$.

   From our historical data analysis, the average value (over all days in the contract period) of a particular day's mean cumulative HDD increment is 13.02, and the average value of the standard deviation of this increment is 3.269.

   The diffusion term therefore has magnitude $\frac{1}{2}\sigma_{T-\tau}^2 \simeq 5$, compared to the convection term which has magnitude $\mu_{T-\tau} \simeq 13$. These values show that our PDE is indeed convection-dominated.

   Taking the minimum value of the diffusion term and the maximum value of the convection term implies that condition (6.8) becomes $\Delta S \leq 0.30$. This is not satisfied by our choice of step-size $\Delta S = 17.5$, but the condition is sufficient and not necessary, and from both Nichols [15] and Figure 6.1 we know that the system does have a unique solution. However, we note that condition (6.8) is equivalent to the cell-Peclet condition (see Anderson [2]):

   $$\left| \frac{\mu_{T-\tau} \Delta S}{\frac{1}{2}\sigma_{T-\tau}^2} \right| \leq 2.$$

Anderson [2] concludes that when this condition is violated (as in our case), the numerical solution produced by the standard central-difference approximation will be oscillatory. This is consistent with the behaviour of our solution apparent from Figure 6.1. To satisfy the cell-Peclet condition for this scheme, that is to enforce $\Delta S \leq 0.82$, is not feasible in practice due to limited computer resources. We will examine alternative methods of dealing with this problem in the next chapter.

2. Another feature of our numerical solution as shown in Figure 6.1 is that a discontinuity exists between the boundary condition $S = 0$ and the solution for $S > 0$. This is due to the fact that the boundary condition $u(0, \tau)$ is not smooth (it is equal to the minimum of a function of τ and the payment cap - see (6.6)), whereas the solution for $S > 0$ is smooth. We will discuss this matter in more detail and consider methods of resolving the issue in the next chapter.

With the exception of these two numerical issues, the evolution of the option value between the initial and boundary conditions, as shown by Figure 6.1, appears reasonable. We see that, as time t increases from 0 to T, S has to increase at an almost constant rate to maintain the same option value. This rate is approximately equal to the average, μ, of the daily drift rates, μ_t, since the PDE is convection-dominated and therefore approximates the wave equation with wave speed μ. Similarly, for a fixed value of S $(0 < S < K)$, the option value increases with time, as the expected value of S at expiry effectively decreases.

Chapter 7

Resolution of Numerical Issues for Cumulative HDD PDE

7.1 Spurious Oscillations

7.1.1 Downwind/Upwind Scheme

As per Morton [12], it is the discretisation of the convection term using central differences that has produced the spurious oscillations in Figure 6.1. This suggests that we should be able to resolve this numerical issue by discretising the convection term using a downwind/upwind scheme. We will therefore implement the Crank-Nicolson scheme with downwind/upwind convection, analysed in Chapter 5. We note from section 5.2 that this scheme is only first order accurate in τ and S. We shall therefore need to use more grid-points for each variable to achieve the same significant figures of accuracy as that in the previous chapter. In addition, this scheme is not unconditionally stable. From section 5.2, we require $\max_{\tau_n} |\mu_{T-\tau_n}|\Delta\tau \leq \Delta S$ for Fourier stability. From our historical temperature data analysis, we have $\max_{\tau_n} |\mu_{T-\tau_n}| = 15.7$, and so we require $15.7\Delta\tau \leq \Delta S$. This is satisfied by the step sizes used in the previous section: $\Delta S = 17.5$ and $\Delta\tau = 1$.

We recall that the Crank-Nicolson scheme with downwind/upwind convection is

$$\begin{aligned}\frac{u_j^{n+1} - u_j^n}{\Delta\tau} &= \frac{1}{2}\left\{\frac{1}{2}\sigma^2_{T-\tau_n}\frac{1}{(\Delta S)^2}(u_{j+1}^n - 2u_j^n + u_{j-1}^n)\right. \\ &\quad \left. + \frac{1}{2}\sigma^2_{T-\tau_{n+1}}\frac{1}{(\Delta S)^2}(u_{j+1}^{n+1} - 2u_j^{n+1} + u_{j-1}^{n+1})\right\} \\ &\quad + \begin{cases} \mu_{T-\tau_n}\frac{1}{\Delta S}\left(u_{j+1}^n - u_j^n\right) \text{ if } \mu_{T-\tau_n} > 0 & \text{(downwind)} \\ \mu_{T-\tau_n}\frac{1}{\Delta S}\left(u_j^n - u_{j-1}^n\right) \text{ if } \mu_{T-\tau_n} < 0 & \text{(upwind).} \end{cases}\end{aligned}$$

Since we are working with cumulative HDD, and HDD are positive by definition, the drift $\mu_{T-\tau_n} \geq 0$, and hence we choose the downwind scheme.

Following the same approach as in section 6.2, if we set

$$\begin{aligned}\lambda_n &= \frac{1}{4}\sigma^2_{T-\tau_n}\frac{\Delta\tau}{(\Delta S)^2}, \quad \text{and}\\ \nu_n &= \mu_{T-\tau_n}\frac{\Delta\tau}{\Delta S},\end{aligned}$$

our problem becomes

$$\mathbf{A}\mathbf{u}^{n+1} = \mathbf{B}\mathbf{u}^n + \mathbf{c}^n,$$

where

$$\mathbf{A} = \begin{pmatrix} 1+2\lambda_{n+1} & -\lambda_{n+1} & 0 & \dots & 0 \\ -\lambda_{n+1} & 1+2\lambda_{n+1} & -\lambda_{n+1} & & \vdots \\ 0 & -\lambda_{n+1} & \ddots & \ddots & 0 \\ \vdots & & \ddots & \ddots & -\lambda_{n+1} \\ 0 & 0 & & -\lambda_{n+1} & 1+2\lambda_{n+1} \end{pmatrix},$$

$$\mathbf{B} = \begin{pmatrix} 1-2\lambda_n-\nu_n & \lambda_n+\nu_n & 0 & \dots & 0 \\ \lambda_n & 1-2\lambda_n-\nu_n & \lambda_n+\nu_n & & \vdots \\ 0 & \lambda_n & \ddots & \ddots & 0 \\ \vdots & & \ddots & \ddots & \lambda_n+\nu_n \\ 0 & 0 & & \lambda_n & 1-2\lambda_n-\nu_n \end{pmatrix},$$

and

$$\mathbf{c}^n = \begin{pmatrix} \lambda_{n+1}u_0^{n+1} + \lambda_n u_0^n \\ 0 \\ \vdots \\ 0 \\ \lambda_{n+1}u_J^{n+1} + (\lambda_n+\nu_n)u_J^n \end{pmatrix},$$

with $\mathbf{u}^n$ and $\mathbf{u}^{n+1}$ defined as before.

Note that in this case we have

$$|-\lambda_{n+1}| + |-\lambda_{n+1}| = 2\lambda_{n+1} < |1+2\lambda_{n+1}|,$$

and therefore the matrix $\mathbf{A}$ is always strictly diagonally dominant and hence non-singular, implying that the system has a unique solution.

We have used the same method as in section 6.2 to solve this tridiagonal system. We used the same HDD step-length ($\Delta S = 17.5$) and time-step (1 day) as in section 6.3.

We can see from Figure 7.1 that the spurious oscillations have been eliminated, as desired.

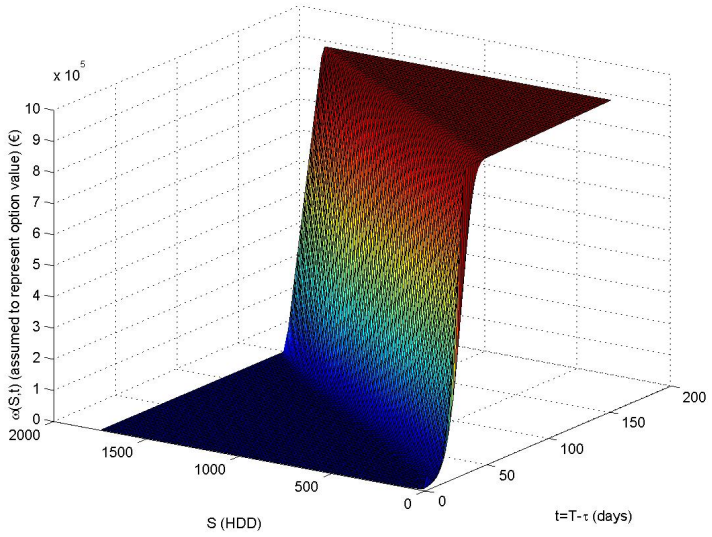

Figure 7.1: Numerical solution of PDE for Cumulative HDD using the Crank-Nicolson method with downwind convection

7.1.2 Semi-Lagrangian Method

Although the downwind scheme implemented in the previous section can be seen to eliminate the spurious oscillations, it is only first order accurate in τ and S. Hence we have lost accuracy in our solution compared to that achieved by the Crank-Nicolson method. Here we will describe and implement the semi-Lagrangian method with monotone interpolation, in an attempt to improve the accuracy of our solution whilst also eliminating spurious oscillations.

Our PDE (6.1) is

$$u_\tau = \frac{1}{2}\sigma^2_{T-\tau} u_{SS} + \mu_{T-\tau} u_S,$$

which can be written as

$$\frac{\partial u}{\partial \tau} - \mu_{T-\tau}\frac{\partial u}{\partial S} = \frac{1}{2}\sigma^2_{T-\tau}\frac{\partial^2 u}{\partial S^2}. \tag{7.1}$$

Using the Chain Rule, we have

$$\frac{du}{d\tau} = \frac{\partial u}{\partial \tau} + \frac{\partial u}{\partial S}\frac{dS}{d\tau}. \tag{7.2}$$

By comparing (7.1) and (7.2), we see that we can write our PDE as the following system of equations:

$$\frac{dS}{d\tau} = -\mu_{T-\tau}, \tag{7.3}$$

$$\frac{du}{d\tau} = \frac{1}{2}\sigma^2_{T-\tau}\frac{\partial^2 u}{\partial S^2}. \tag{7.4}$$

We use a grid, as before, with $u_j^n \simeq u(S_j, \tau_n)$, where $S_j = j\Delta S$, $\tau_n = n\Delta\tau$. To construct a semi-Lagrangian scheme, we begin by assuming that the solution is known at $\tau = \tau_n$, and make a forward step in τ using the method of characteristics. We wish to find the finite difference solution u_j^{n+1} at each grid point $S_j = j\Delta S$.

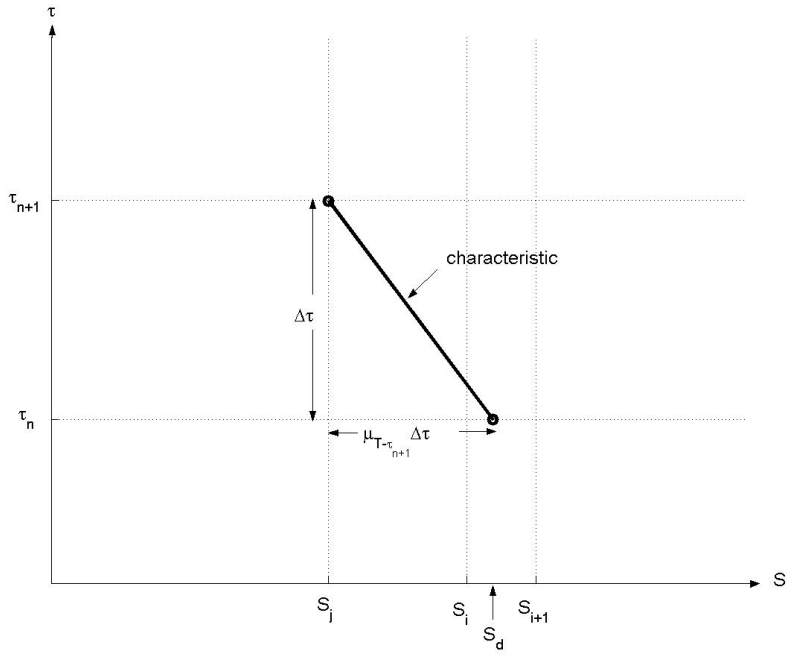

Figure 7.2: Construction of the semi-Lagrangian method

The characteristic is a straight line with gradient $\frac{d\tau}{dS}$, which from (7.3) is given by

$$\begin{aligned} \frac{d\tau}{dS} &= -\frac{1}{\mu_{T-\tau}} \\ &= -\frac{1}{\mu_{T-\tau_{n+1}}} \text{ at } \tau = \tau_{n+1}. \end{aligned}$$

We extend this characteristic from τ_{n+1} back to τ_n, where it passes through the departure point S_d. (See Figure 7.2).

We can therefore calculate S_d by

$$S_d = S_j + \mu_{T-\tau_{n+1}}\Delta\tau.$$

We then apply the "Crank-Nicolson" scheme to equation (7.4), to obtain

$$\begin{aligned} \frac{u_j^{n+1} - u_d^n}{\Delta\tau} &= \frac{1}{2}\left\{\frac{1}{2}\sigma^2_{T-\tau_n}\frac{1}{(\Delta S)^2}(u_{j+1}^n - 2u_j^n + u_{j-1}^n)\right. \\ &\quad \left. + \frac{1}{2}\sigma^2_{T-\tau_{n+1}}\frac{1}{(\Delta S)^2}(u_{j+1}^{n+1} - 2u_j^{n+1} + u_{j-1}^{n+1})\right\}, \end{aligned} \tag{7.5}$$

where u_d^n is the approximation to u at the departure point (S_d, τ_n).

Generally S_d will not lie on a grid-point of S, and therefore interpolation will be required to evaluate u_d^n.

We will start by using linear interpolation:

$$u_d^n = \left(\frac{S_d - S_i}{\Delta S}\right) u_{i+1}^n + \left(\frac{S_{i+1} - S_d}{\Delta S}\right) u_i^n,$$

where S_d lies between grid points S_i and S_{i+1}.

If we write this as

$$u_d^n = \alpha_j^n u_{i+1}^n + \beta_j^n u_i^n,$$

where $\alpha_j^n = \left(\frac{S_d - S_i}{\Delta S}\right)$, $\beta_j^n = \left(\frac{S_{i+1} - S_d}{\Delta S}\right)$, our scheme (7.5) becomes

$$\begin{aligned}\frac{u_j^{n+1} - \alpha_j^n u_{i+1}^n - \beta_j^n u_i^n}{\Delta\tau} = \frac{1}{2}\Bigg\{ & \frac{1}{2}\sigma^2_{T-\tau_n}\frac{1}{(\Delta S)^2}(u_{j+1}^n - 2u_j^n + u_{j-1}^n) \\ & + \frac{1}{2}\sigma^2_{T-\tau_{n+1}}\frac{1}{(\Delta S)^2}(u_{j+1}^{n+1} - 2u_j^{n+1} + u_{j-1}^{n+1})\Bigg\}.\end{aligned}$$

Following the same approach as in section 7.1.1, if we set

$$\lambda_n = \frac{1}{4}\sigma^2_{T-\tau_n}\frac{\Delta\tau}{(\Delta S)^2},$$

our problem becomes

$$\mathbf{A}\mathbf{u}^{n+1} = \mathbf{B}\mathbf{u}^n + \mathbf{c}^n + \mathbf{d}^n,$$

where

$$\mathbf{A} = \begin{pmatrix} 1+2\lambda_{n+1} & -\lambda_{n+1} & 0 & \dots & 0 \\ -\lambda_{n+1} & 1+2\lambda_{n+1} & -\lambda_{n+1} & & \vdots \\ 0 & -\lambda_{n+1} & \ddots & \ddots & 0 \\ \vdots & & \ddots & \ddots & -\lambda_{n+1} \\ 0 & 0 & & -\lambda_{n+1} & 1+2\lambda_{n+1} \end{pmatrix},$$

$$\mathbf{B} = \begin{pmatrix} -2\lambda_n & \lambda_n & 0 & \dots & 0 \\ \lambda_n & -2\lambda_n & \lambda_n & & \vdots \\ 0 & \lambda_n & \ddots & \ddots & 0 \\ \vdots & & \ddots & \ddots & \lambda_n \\ 0 & 0 & & \lambda_n & -2\lambda_n \end{pmatrix},$$

$$\mathbf{c}_j^n = \alpha_j^n u_{i+1}^n + \beta_j^n u_i^n,$$

and

$$\mathbf{d}^n = \begin{pmatrix} \lambda_{n+1} u_0^{n+1} + \lambda_n u_0^n \\ 0 \\ \vdots \\ 0 \\ \lambda_{n+1} u_J^{n+1} + \lambda_n u_J^n \end{pmatrix},$$

with $\mathbf{u}^n$ and $\mathbf{u}^{n+1}$ defined as before.

Note that, as for the downwind scheme, the matrix $\mathbf{A}$ is always strictly diagonally dominant and hence non-singular, implying that the system has a unique solution.

We have used the same method as in sections 6.2 and 7.1.1 to solve this tridiagonal system, with the same HDD step-length ($\Delta S = 17.5$) and time-step (1 day).

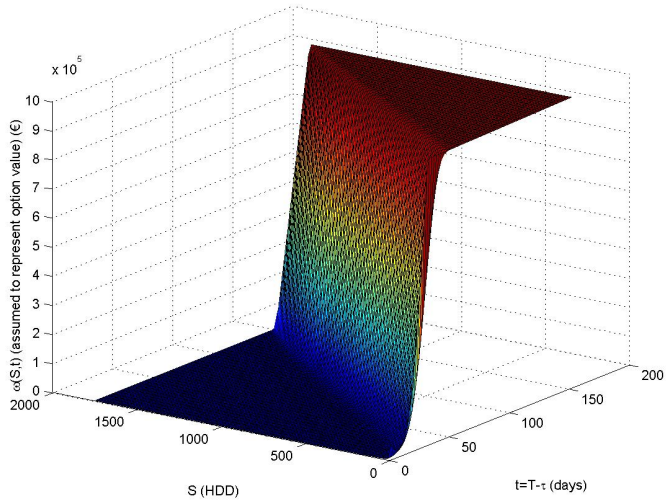

Figure 7.3: Numerical solution of PDE for Cumulative HDD using the semi-Lagrangian method with linear interpolation

We can see from Figure 7.3 that, as for the downwind scheme, the spurious oscillations seen in Figure 6.1 have been eliminated. The order of accuracy of the scheme is not apparent from the graph of the numerical solution. However, as per Smith [17], and Garcia-Navarro and Priestley [7], the use of linear interpolation in a semi-Lagrangian scheme only results in first order accuracy, since the resulting scheme can be recast as a first order upwind difference method. So far, therefore, we have not improved upon the downwind scheme in section 7.1.1.

However, it is well known that the accuracy of the semi-Lagrangian scheme can be increased by using monotone cubic interpolation rather than linear interpolation. (See Garcia-Navarro and Priestley [7]). The cubic polynomial is required to be monotone to avoid problems at large gradients. (See Priestley [16]).

Garcia-Navarro and Priestley [7] suggests the use of a Hermite cubic polynomial

$$u_d^n = p(S_d) = c_1(S_d - S_i)^3 + c_2(S_d - S_i)^2 + c_3(S_d - S_i) + c_4,$$

where the coefficients are

$$\begin{aligned} c_1 &= \frac{d_{i+1} + d_i - 2\Delta_i}{(\Delta S)^2}, \\ c_2 &= \frac{-d_{i+1} - 2d_i + 3\Delta_i}{\Delta S}, \\ c_3 &= d_i, \\ c_4 &= u_i^n. \end{aligned}$$

Here Δ_i is the discrete slope between grid point S_i and S_{i+1}, defined as

$$\Delta_i = \frac{u_{i+1}^n - u_i^n}{\Delta S},$$

and d_i is the S derivative of u at $S = S_i$, $\tau = \tau_n$, which can be estimated by

$$d_i = \frac{-\Delta_{i-2} + 7\Delta_{i-1} + 7\Delta_i - \Delta_{i+1}}{12}$$

for an interior point. Slightly different formulae are applied to the points which do not have two neighbours (d_0, d_1, d_{J-1} and d_J).

We note that the above definitions give us

$$\begin{aligned} p(S_i) &= u_i^n, \\ p(S_{i+1}) &= u_{i+1}^n, \\ p'(S_i) &= d_i, \\ p'(S_{i+1}) &= d_{i+1}, \end{aligned}$$

as desired.

As per Garcia-Navarro and Priestley [7], the monotonicity of this cubic interpolant is enforced by first imposing a necessary condition on the value of the derivatives:

$$\begin{cases} \text{sign}(d_i) = \text{sign}(\Delta_i) = \text{sign}(d_{i+1}), & \Delta_i \neq 0 \\ d_i = d_{i+1} = 0, & \Delta_i = 0, \end{cases}$$

and then limiting their values such that

$$d_i = \text{sign}(d_i)\min(|d_i|, |3\Delta_{i-1}|, |\Delta_i|).$$

Figure 7.4 shows the result of implementing this monotone cubic interpolation with $\Delta S = 17.5$ and a time-step of 1 day.

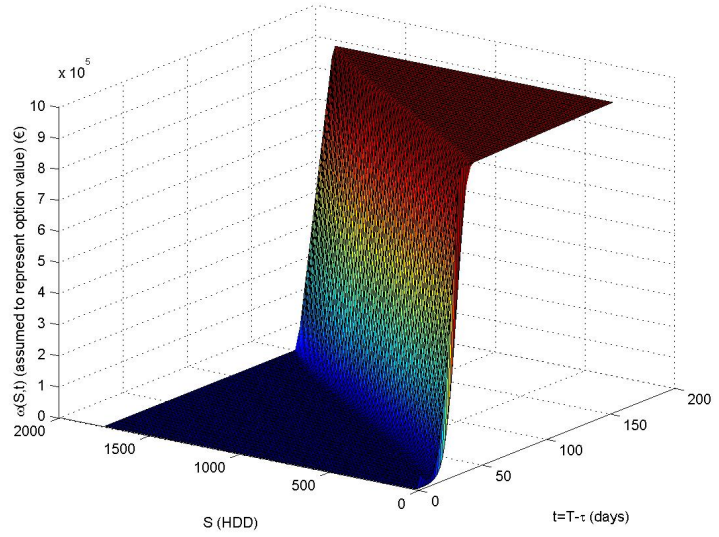

Figure 7.4: Numerical solution of PDE for Cumulative HDD using the semi-Lagrangian method with monotone cubic interpolation

7.1.3 Accuracy Testing

Since the order of accuracy of the downwind and semi-Lagrangian (with linear/cubic interpolation) schemes is not apparent from the numerical solution graphs in Figures 7.1, 7.3 and 7.4, we have used the numerical results to perform some accuracy testing. We have chosen four representative points on the $S - t$ grid, and for each scheme, calculated the average value of ω at these points when the number of cumulative HDD steps $J = \frac{K}{\Delta S} = 8$, 16, 32 and 64 (using $\Delta\tau$=1 day). From the previous theory, the semi-Lagrangian scheme with monotone cubic interpolation should be the most accurate. We have therefore taken the average value of ω produced by this scheme for J=64 to be the 'exact' solution, and hence calculated a representative absolute error of the solution produced by each scheme for J=8, 16, 32 and 64.

Figure 7.5 shows the natural logarithm of the representative absolute error ϵ plotted against the natural logarithm of the cumulative HDD step-length ΔS for each scheme. For a scheme that is pth order accurate in S, we should find that

$$\epsilon \propto (\Delta S)^p,$$

and hence that

$$\ln(\epsilon) = p \ln(\Delta S) + c,$$

where c is a constant. This implies that the gradients of the lines in Figure 7.5 should approximate the order of accuracy in S of the respective schemes.

Since order of accuracy is an asymptotic result, we are really interested in the gradient of the lines for very small ΔS. However, in practice, we are unable to obtain the numerical solution of the PDE for small ΔS, as we are restricted by the availability of

computing resources, and by the conditional stability of the downwind scheme (since we are fixing $\Delta\tau = 1$ day). It can be seen from Figure 7.5 that the lines for the downwind scheme and semi-Lagrangian scheme with linear interpolation have almost unit gradient, which appears to be consistent with our previous assertion that these two schemes are first order accurate in S. The gradient of the line for the semi-Lagrangian scheme with monotone cubic interpolation appears to have a slightly greater gradient, indicating consistency with the theory that this scheme has a higher order of accuracy. However, for more conclusive results, we would need to perform this analysis for smaller ΔS, which would require greater computing resources and the use of a smaller $\Delta\tau$ (for stability of the downwind scheme). We have not decreased $\Delta\tau$ beyond 1 day because our historical temperature data is only defined on a daily basis. Further refinement of the time-step would be possible if interpolation of the daily historical data were performed, but this is beyond the scope of this dissertation. (See section 10.3.)

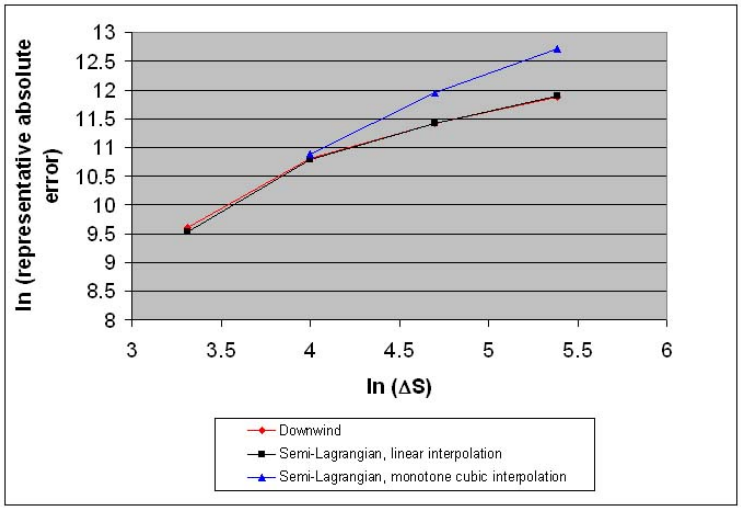

Figure 7.5: Representative absolute error for downwind and semi-Lagrangian schemes

7.2 Discontinuity at $S = 0$

The boundary condition $u(0, \tau)$ given by equation (6.6) is shown graphically in Figure 7.6. We can see that this boundary condition is not smooth, in that the first derivative u_τ does not exist at $\tau = 119$ ($t = 32$) days. However for $S > 0$, the solution $u(S, \tau)$ is smooth as u_τ exists for all τ. This has resulted in a discontinuity between the solution for $S = 0$ and that for $S > 0$, apparent from Figures 6.1, 7.1, 7.3 and 7.4. (Recall that our solution is given by $\omega(S, \tau) = e^{-r\tau}u(S, \tau)$.)

We observe that since the one-sided first derivative u_τ changes suddenly at $(S = 0, t = 32)$, the second derivative $u_{\tau\tau}$ does not exist at this point. It is therefore likely that $u_{\tau\tau}$ will be large along the start of the 'ridge' that evolves from this point for $S > 0$ (running from $(S = 0, t = 32)$ to $(S = 1750, t = 151)$). (See Figure 6.1.) Similarly we

may expect $u_{\tau\tau\tau}$ and higher derivatives to be large in the same region. This means that the Taylor series expansion of the truncation error for the Crank-Nicolson scheme (see equation (5.9)) does not decrease term by term, and so we cannot neglect higher order terms. This is also the case for the Taylor series expansions of the truncation error for the downwind and semi-Lagrangian schemes. It is therefore possible that all of these schemes will lose accuracy in this region.

One possible approach to resolving this issue would be to refine our grid (decrease the cumulative HDD step-length and the time-step) around the point $(S = 0, t = 32)$ and also around the ridge that runs from $(S = 0, t = 32)$ to $(S = 1750, t = 151)$. However since this ridge is not fixed in S or t, an irregular grid of this form would be very difficult to construct in practice. (See section 10.3.) Also, as mentioned in the previous section, decreasing the time-step beyond one day would require interpolation of the historical temperature data, which is not within the scope of this dissertation.

We could also consider using an irregular grid where the ridge running from $(S = 0, t = 32)$ to $(S = 1750, t = 151)$ was taken to be one of the grid lines. However this is complicated by the fact that the drift μ_t and volatility σ_t change on each time-step, so the ridge itself is not a straight line. (See section 10.3.)

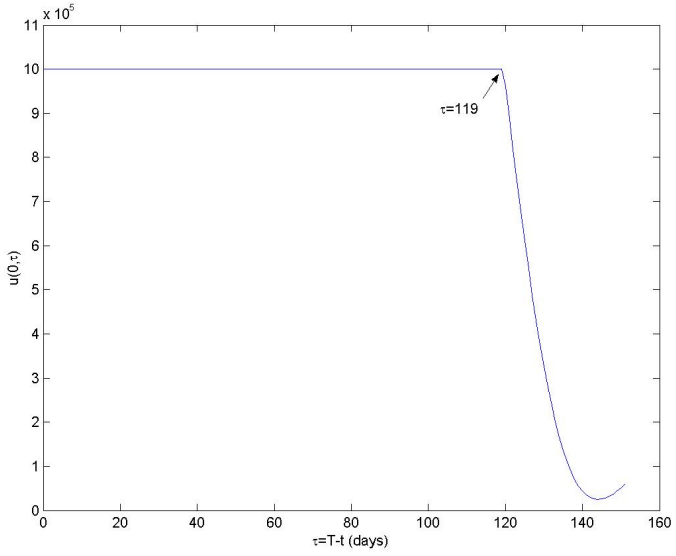

Figure 7.6: Boundary condition $u(0, \tau)$ for Cumulative HDD PDE

Chapter 8

Solution of the PDE for Temperature

8.1 Introduction

We again consider the general PDE set out in equation (4.20) of Chapter 4, but this time assume that the independent variable z represents temperature. We therefore replace z by X, and the PDE becomes

$$u_\tau = \frac{1}{2}\sigma^2_{T-\tau} u_{XX} + \mu_{T-\tau} u_X. \tag{8.1}$$

To be consistent with the PDE for cumulative HDD, we would like our initial condition to take the form

$$u(X, 0) = P(X),$$

where $P(X)$ is the option payoff. However, the option payoff at expiry does not depend on the temperature X at the expiry date; instead it depends on the cumulative HDD at expiry. We therefore need to include the variable S (cumulative HDD) in our solution for u, and the initial condition then becomes

$$u(X, S, 0) = P(S) = \min\left\{\max(K - S, 0) \times tick, cap\right\}. \tag{8.2}$$

From (4.22) and (4.23), assuming that u is a function of S as well as of X and τ, our boundary conditions take the form

$$\begin{aligned} u(X_1, S, \tau) &= e^{r\tau} B_1, \quad \text{and} \\ u(X_2, S, \tau) &= e^{r\tau} B_2, \end{aligned}$$

where B_1 and B_2 are the option values at $X = X_1$ and $X = X_2$ respectively.

To derive these boundary conditions, we consider the two extreme cases:

1. As $X \to -\infty$, the cumulative number of HDD, $S \to \infty$ which means that $K - S < 0$ and so the payoff from the option will be zero. This implies that the value of the option at time $t = T - \tau$ must be zero.
   Therefore we have $X_1 = -\infty,\ B_1 = 0$.

2. As $X \to +\infty$, the contract period is assumed to be so warm, and hence the cumulative number of HDD, S, so small that $(K - S) \times tick > cap$, and so the payoff from the option will be the payment cap. This implies that the value of the option at time $t = T - \tau$ must be $e^{-r\tau} cap$.
   Therefore we have $X_2 = +\infty,\ B_2 = e^{-r\tau} cap$.

Hence the boundary conditions are

$$u(-\infty, S, \tau) = 0, \quad \text{and} \tag{8.3}$$
$$u(+\infty, S, \tau) = cap. \tag{8.4}$$

Here we are assuming that $\omega(X, S, \tau) = e^{-r\tau} u(X, S, \tau)$ may be assumed to represent the value of the option at time $t = T - \tau$ when the temperature is equal to X and the cumulative HDD equal to S, for the reasons outlined in section 4.3.

8.2 Numerical Solution

We wish to solve PDE (8.1) with initial and boundary conditions (8.2), (8.3) and (8.4). It may appear that we have to solve for u as a function of three independent variables, X, S, and τ. However, what we actually have is akin to a discretely-sampled Asian option, where the option payoff depends on a discretely-measured (on a daily basis in our case) arithmetic average or running sum of the underlying (cumulative HDD being a modified running sum of temperature). There is a recognised strategy for valuing such an option (see Wilmott *et al* [18], [19] and Zvan *et al* [20]), which we apply to our problem as follows:

1. Our option value depends on the cumulative HDD

$$S = \sum_{i=1}^{N} \max(18 - X_i, 0), \tag{8.5}$$

   where X_i is the average temperature on day i, and N is the number of days in the contract period (151 for our example contract detailed in section 1.3).

   S is updated discretely, and is therefore constant between the daily sampling points. This implies that, between the daily sampling points, the PDE for the option value is simply (8.1) with S treated as a parameter.

   We therefore start at $\tau = 0$ ($t = T$), where the option value is given by initial condition (8.2), and step forwards in τ (backwards in time t), solving PDE (8.1) between daily sampling points. On each step we use the value of the option immediately after the previous daily sampling point as initial data. This gives the value of the option until immediately before the current daily sampling point. Between sampling points, we solve the PDE using the Crank-Nicolson scheme implemented in the same way as that described in section 6.2, but with the boundary conditions (8.3) and (8.4).

2. At the current daily sampling point, the value of S is updated. If S_n is the cumulative number of HDD at day n, from definition (8.5), we have

$$S_n = S_{n-1} + \max(18 - X_n, 0). \tag{8.6}$$

We assume, when valuing an option, that there are no riskless arbitrage opportunities (see Hull [9]). This means that the option price can not change discontinuously. In particular, the option value must be continuous across a daily sampling point. If we consider a sampling point t_n, we must therefore have the condition

$$u(X_n, S_n, t_n^+) = u(X_n, S_{n-1}, t_n^-),$$

where t_n^- and t_n^+ are the values of time t immediately before and after the sampling point. Rewriting this in terms of $\tau = T - t$ for the purpose of solving our PDE, we obtain

$$u(X_{N-n}, S_{N-n-1}, \tau_n^+) = u(X_{N-n}, S_{N-n}, \tau_n^-)$$

at sampling date τ_n.

Substituting from (8.6), and assuming that X is continuous and takes the same value immediately before and immediately after sampling, this becomes

$$u(X, S_{N-n-1}, \tau_n^+) = u(X, S_{N-n-1} + \max(18 - X, 0), \tau_n^-).$$

Since S_{N-n-1} does not change from τ_n^+ to τ_{n+1}^-, we can drop its suffix, and arrive at the 'jump' condition

$$u(X, S, \tau_n^+) = u(X, S + \max(18 - X, 0), \tau_n^-). \tag{8.7}$$

We apply this jump condition at the current daily sampling point to deduce the value of the option immediately after the present sampling date.

3. Note that u depends on the value of S up to $N \times \max(\max(18 - X, 0))$, or equivalently, up to $N \times (18 - \min(X))$. If we take the minimum temperature X to be $-50\,^\circ\mathrm{C}$, say, this gives us a maximum value of S of 10268 (for $N = 151$).

We will only be considering a range of X of magnitude $-50 \leq X \leq 50$, compared to a range of S of magnitude $0 \leq S \leq 10268$. It is not therefore computationally feasible to make ΔS as small as ΔX. This means that, in applying jump condition (8.7), $S + \max(18 - X, 0)$ may not fall on a grid point of S. In this case we use linear interpolation to approximate the value of u at $S + \max(18 - X, 0)$.

We first find grid points S_i and S_{i+1}, where $S_i = i\Delta S$, such that

$$S_i < S + \max(18 - X, 0) < S_{i+1}.$$

We then have

$$u(X, S + \max(18 - X, 0), \tau) = u(X, S_i, \tau) + \left\{ \left(\frac{u(X, S_{i+1}, \tau) - u(X, S_i, \tau)}{S_{i+1} - S_i} \right) \times (S + \max(18 - X, 0) - S_i) \right\}.$$

This linear interpolation can be shown to be accurate to $O((\Delta S)^2)$ for smooth u. This is consistent with the second order accuracy in X and τ achieved by the Crank-Nicolson scheme (see Chapter 5).

4. We repeat this process as necessary to arrive at the value of our option at time $t = 0$ ($\tau = T$). Since we are solving the PDE on a three-dimensional grid ($X \times S \times \tau$), we can not use this method to provide graphical information about the evolution of the option value (we would require a four-dimensional surface). However, since we know that at time $t = 0$ we must have $S = 0$ (S is cumulative), by setting $S = 0$, we can obtain the value of the option at $t = 0$ in terms of the initial temperature X_0.

In solving this PDE numerically, we calculate the temperature volatility and drift, $\sigma_{T-\tau}$ and $\mu_{T-\tau}$ respectively, by applying the same method as that used to calculate the cumulative HDD volatility and drift in Chapter 6. We use the approximation of equation (4.2):

$$X_{t+\Delta t} - X_t \sim N(\mu_t \Delta t, \sigma_t \sqrt{\Delta t}), \tag{8.8}$$

combined with our analysis of historical daily temperature increments in Chapter 2.

For $\Delta t = 1$ day, equation (8.8) becomes

$$X_{t+1} - X_t \sim N(\mu_t, \sigma_t).$$

This tells us that

$\mu_t = \mu_{T-\tau}$ = the mean of the daily increment $X_{t+1} - X_t$, and
$\sigma_t = \sigma_{T-\tau}$ = the standard deviation of the daily increment $X_{t+1} - X_t$.

From our historical data analysis, the average value (over all days in the contract period) of a particular day's EWMA mean temperature increment is -0.0252, and the average value of the EWMA standard deviation of this increment is 0.2285.

The diffusion term therefore has magnitude $\frac{1}{2}\sigma_{T-\tau}^2 \simeq 0.03$, compared to the convection term which has magnitude $\mu_{T-\tau} \simeq -0.03$. These values show that our PDE for temperature has diffusion and convection terms of the same absolute magnitude, but is not convection-dominated. We therefore do not expect to observe spurious oscillations to the same extent as those produced by the convection-dominated cumulative HDD PDE. (See section 6.3.)

Also in this case, the sufficient condition (6.8) for the tridiagonal matrix system to have a unique solution becomes $\Delta X \leq 2.07$, which is easy to satisfy in practice (see

the next section). As remarked in section 6.3, condition (6.8) is equivalent to the cell-Peclet condition, which when violated, causes the numerical solution produced by the standard central-difference approximation to be oscillatory. Therefore, by satisfying this condition, we should be able to prevent spurious oscillations from occurring in our solution.

8.3 Results

We have applied the previous methodology to solve PDE (8.1) with initial and boundary conditions (8.2), (8.3) and (8.4) for the example contract in section 1.3. We used a temperature step-length of $\Delta X = 0.2$ (500 temperature steps, since we are assuming $-50 \leq X \leq 50$), a cumulative HDD step-length of $\Delta S = 4$ (2567 HDD steps, since we have $0 \leq S \leq 10268$) and a time-step of 1 day (151 time-steps, since $T = 151$ days).

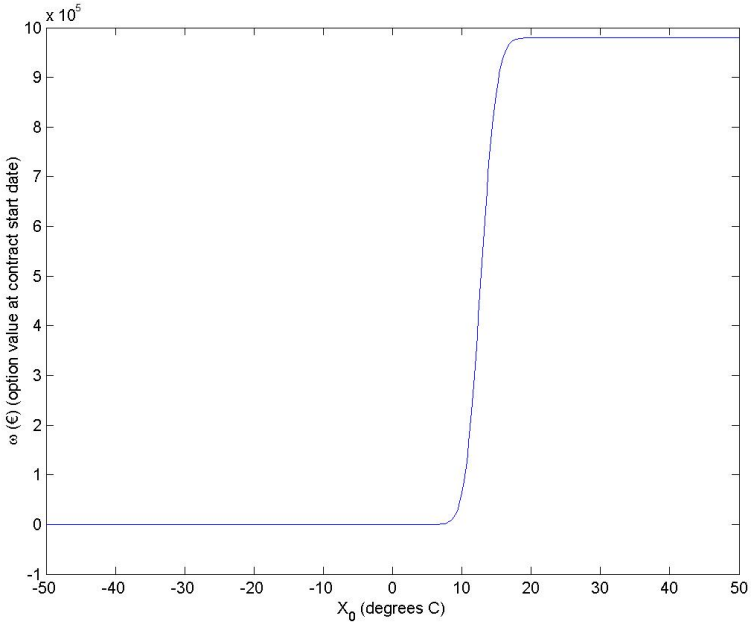

Figure 8.1: Numerical solution of PDE for temperature: $t = 0, S = 0$

From our historical temperature data, the mean (over the last fifty years) of the average temperature X on 31 October (time $t = 0$) is 9.9 °C. From Figure 8.1, we therefore read off the value of ω when $X_0 = 9.9$ to give us our initial option value to be 57,524 Euros. This is consistent with the value of 58,415 Euros obtained in Chapter 3 using the expectation-based approach.

We observe from Figure 8.1 that the gradient $\frac{d\omega}{dX_0}$ is very large in the region $8 \leq X_0 \leq 18$. In particular, we can calculate the value of this gradient to be 64,413 Euros/°C at $X_0 = 9.9$. This implies that the option value produced by this method is extremely sensitive to the initial temperature of the period.

The following table shows the effect of refining the temperature and cumulative HDD step-length (for a time-step of 1 day):

ΔX (°C)	ΔS (°C)	Option value (Euros)
0.2	4	57,524
0.2	2	57,189
0.2	1	57,096
0.1	2	57,566
0.1	1	57,475

For a fixed number of daily sampling points, we know that the combination of our Crank-Nicolson method and linear interpolation should result in a global discretisation error of

$$O((\Delta\tau)^2) + O((\Delta X)^2) + O((\Delta S)^2).$$

We can see from the previous table that the option value only changes by 49 Euros in going from the coarsest to the finest grid. This implies that the absolute value of our global discretisation error is not unduly significant for a fixed time-step $\Delta\tau$. Investigation of refining the time-step is beyond the scope of this dissertation. (See section 10.3.)

Chapter 9

Monte Carlo Simulations and Other Valuation Methods

9.1 Monte Carlo Simulations

'Monte Carlo' is a computer-based technique for generating random numbers, which can be used to statistically construct weather scenarios. For our example contract, it involves generating a large number of simulated scenarios of HDD to determine the possible payoffs for the option at expiry. The value of the option is then calculated as being the discounted average of all simulated payoffs.

To simulate the scenarios of HDD, we will use SDE (4.1):

$$dZ_t = \mu_t dt + \sigma_t dW_t,$$

where Z_t is either the cumulative HDD or the temperature at time t.

We will choose to model temperature, since from Chapter 2, daily temperature increments fit a normal distribution more closely than daily cumulative HDD increments, and therefore the temperature process should be the more accurate. (See equation (4.2)).

Using X_t to represent the temperature at time t, we therefore have

$$dX_t = \mu_t dt + \sigma_t dW_t.$$

Discretising using the Euler method, we obtain

$$X_{t+\Delta t} - X_t = \mu_t \Delta t + \sigma_t (W_{t+\Delta t} - W_t),$$

or

$$X_{t+\Delta t} - X_t = \mu_t \Delta t + \sigma_t \epsilon \sqrt{\Delta t}, \tag{9.1}$$

where $\epsilon \sim N(0,1)$, by the definition of the standard Wiener process.

We use $X_0 = 9.9$ (the mean of the daily average temperature at $t = 0$), and step

forward in time increments of $\Delta t = 1$ day using equation (9.1). Since (9.1) implies that

$$X_{t+1} - X_t \sim N(\mu_t, \sigma_t),$$

we calculate μ_t as being the (EWMA) mean of the daily temperature increment $X_{t+1} - X_t$ and σ_t as being the (EWMA) standard deviation (using the historical temperature data). We compute ϵ by taking a random drawing from the standard normal distribution. Using these inputs we construct a temperature path for the length of the contract.

We have run $50,000$ such simulations, for each one calculating the daily HDD and hence the cumulative HDD and payoff at expiry. We have averaged these payoffs and discounted the average to give a value for our option at time $t = 0$. Figure 9.1 shows five of these simulations.

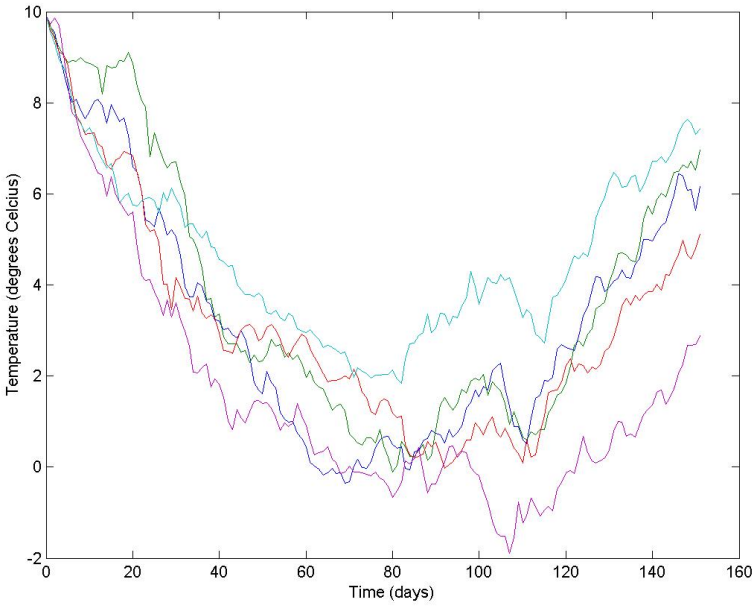

Figure 9.1: Monte Carlo temperature simulations

The above method gives the option value at time $t = 0$ to be $55,630$ Euros. This supports the results obtained using the expectation and PDE approaches in Chapters 3 and 8 respectively.

9.2 Other Valuation Methods

9.2.1 Burn Analysis

This method values the weather derivative based on the payoff that would have been obtained if the contract had been held in the past. (See Nelken [14]). After collection

of the historical temperature data and any necessary corrections (see section 2.3), the steps are:

1. For each year in the past, determine what the option would have paid out.
2. Find the average of these payoff amounts.
3. Discount back to the valuation date (the contract start date).

Burn analysis values our example contract from section 1.3 at 42,843 Euros, lower than the values obtained in our previous methods.

However this method is clearly very simplistic, and is likely to be inaccurate without considerable 'cleansing' of the historical data. If a temperature anomaly occurs in any year (whether from extreme weather conditions or from errors in the data), the use of Burn Analysis means that this anomaly may have a significant effect on the valuation of the weather derivative. This is more of an issue for Burn Analysis than for the expectation approach in Chapter 3, since the former gives each historical year's data an equal weighting, whereas the latter smooths the historical data by fitting it to a normal distribution curve.

9.2.2 Use of Weather Forecasts

The valuation methods described and implemented in this dissertation have not taken any meteorological forecasts into account. The values determined by these methods can be assumed (after appropriate discounting is applied) to hold at times well before the start of the contract period, since meteorologists generally believe that temperature predictions more than a week or so in advance are not very significant.

However as we approach the start of the contract period, we should adjust the parameters of our valuation model (i.e. the mean and standard deviation of the cumulative HDD or of the daily increments in cumulative HDD / average temperature) to incorporate information obtained from recent forecasts. For example, if we believe that the temperature will be higher than normal during the contract period, we should decrease the mean of the cumulative HDD used in the expectation approach of Chapter 3.

Chapter 10

Conclusions and Further Research

10.1 Summary of Results

We have shown that, if the daily increments in cumulative HDD and average temperature are assumed to be normally distributed (which appears reasonable from our analysis of historical temperature data), we can formulate an SDE and use this to derive a convection-diffusion PDE with time-dependent coefficients for the value of an HDD put option. When the underlying process is cumulative HDD, we have found this PDE to be convection-dominated. In this case our preferred numerical solution technique is the semi-Lagrangian method with monotone cubic interpolation. Also in this case, we have found that, if we assume cumulative HDD themselves to be normally distributed (consistent with our historical data analysis), we can use expectation theory to derive a valuation result which can be applied as a boundary condition for the PDE. When the underlying process is temperature, we have found the PDE to have convection and diffusion terms of similar magnitude, and discovered that we can solve this numerically as a discretely-sampled Asian option, using the Crank-Nicolson scheme between sampling points.

The table below summarises the results obtained for the value of our example contract in section 1.3, from the numerical solution of our PDE as well as from more traditional methods.

Method	Option value (Euros) at the contract start date
PDE	
-for cumulative HDD [1]	58,415
-for temperature [2]	57,475
Monte Carlo Simulation	55,630
Burn Analysis	42,843

[1] with boundary condition derived using expectation theory
[2] for the smallest grid size investigated

With the exception of Burn Analysis, which we know is very simplistic and likely to be inaccurate, the above methods give very similar results for the value of our HDD put option at the contract start date. This demonstrates that the numerical solution of our PDE can be used to give reasonably accurate results for the value of our weather derivative.

10.2 Benefits and Limitations of our PDE Method

The numerical schemes used to solve the PDE all introduce a degree of error (although so too does the discretisation used in the Monte Carlo simulation). The accuracy of our numerical solutions has also been restricted by the fact that our historical temperature data and therefore our drift and volatility parameters are only defined on a daily basis, and so, without performing interpolation of the daily historical data, we have not been able to use a time-step of less than one day. In addition, the value of the option at the contract start date using the PDE for cumulative HDD is just that given by expectation theory, and the numerical solution of the PDE for temperature is extremely sensitive to the initial temperature of the contract period.

However, we have hypothesised that the solution of our PDE for cumulative HDD represents the evolution of the option value. Hence it appears that this method may be used to gain information about the value of the option during the contract period. This is a distinct advantage of the PDE method over traditional methods which tend to value the derivative at one point in time only.

10.3 Further Research

Further work would be required to establish that the solution of our cumulative HDD PDE does indeed represent the evolution of our option value. We could also improve this solution by local grid refinement or the use of an irregular grid, to resolve the numerical issue of the discontinuity discussed in section 7.2.

It would be beneficial to examine methods of interpolating the daily historical temperature data, to enable time-steps of less than one day to be used in the numerical schemes. Assuming that an interpolation method of a sufficiently high order of accuracy could be used, this would increase the accuracy of our numerical solutions.

In addition we could consider developing, analysing and solving numerically PDE's for more physically realistic stochastic temperature processes, such as the mean-reverting processes proposed in Brody *et al* [4] and Alaton *et al* [1].

Appendix A

Itô's Lemma in Integral Form

We quote the version of Itô's Lemma given in Neftci [13]. This is applied in the derivation of the PDE in section 4.2.

Let $F(S_t, t)$ be a twice-differentiable function of t and of the random process S_t:

$$dS_t = \mu_t dt + \sigma_t dW_t, \qquad t \geq 0, \tag{A.1}$$

where dW is a standard Wiener process and μ_t, σ_t are well-behaved drift and diffusion parameters.

Alternatively, in integral form, the random process can be written as

$$S_t = S_0 + \int_0^t \mu_u du + \int_0^t \sigma_u dW_u.$$

Then Itô's Lemma states that

$$dF = \frac{\partial F}{\partial S_t} dS_t + \frac{\partial F}{\partial t} dt + \frac{1}{2} \frac{\partial^2 F}{\partial S_t^2} \sigma_t^2 dt. \tag{A.2}$$

Substituting for dS_t from equation (A.1), equation (A.2) becomes

$$dF = \left(\frac{\partial F}{\partial S_t} \mu_t + \frac{\partial F}{\partial t} + \frac{1}{2} \frac{\partial^2 F}{\partial S_t^2} \sigma_t^2 \right) dt + \frac{\partial F}{\partial S_t} \sigma_t dW_t. \tag{A.3}$$

Integrating both sides of (A.3), we obtain

$$F(S_t, t) = F(S_0, 0) + \int_0^t \left[F_s \mu_u + F_u + \frac{1}{2} F_{ss} \sigma_u^2 \right] du + \int_0^t F_s \sigma_u dW_u. \tag{A.4}$$

Bibliography

[1] Alaton, P., Djehiche, B. and Stillberger, D. *On Modelling and Pricing Weather Derivatives*. 2001.

[2] Anderson, D.A., Tannehill, J.C. and Pletcher, R.H. *Computational Fluid Mechanics and Heat Transfer*. Hemisphere Publishing Corporation, New York 1984.

[3] Black, F. and Scholes, M. *The Pricing of Options and Corporate Liabilities*. Journal of Political Economy 1973.

[4] Brody, D.C., Syroka, J. and Zervos, M. *Dynamical Pricing of Weather Derivatives*. Quantitative Finance Volume 2 (2002) 189-198, Institute of Physics Publishing.

[5] Clewlow, L. and Strickland, C. *Energy Derivatives: Pricing and Risk Management*. Lacima Publications 2000.

[6] Dischel, B. *Black-Scholes Won't Do*. Weather Risk 2003.

[7] Garcia-Navarro, P. and Priestley, A. *A Conservative and Shape-Preserving Semi-Lagrangian Method for the Solution of the Shallow Water Equations*. Numerical Analysis Report 6/93. University of Reading 1993.

[8] Garman, M., Blanco, C. and Erickson, R. *Weather Derivatives: Instruments and Pricing Issues*. Environmental Finance 2000.

[9] Hull, J.C. *Options, Futures, and Other Derivatives*. Prentice Hall International, Inc. 1997.

[10] Jäckel, P. *Monte Carlo Methods in Finance*. Wiley 2002.

[11] McIntyre, R. *Black-Scholes Will Do*. Energy and Power Risk Management 1999.

[12] Morton, K.W. *Numerical Solution of Convection-Diffusion Problems*. Chapman & Hall 1996.

[13] Neftci, S.N. *An Introduction to the Mathematics of Financial Derivatives*. Academic Press 2000.

[14] Nelken, I. *Weather Derivatives - Pricing and Hedging*. Super Computer Consulting, Inc. 2000.

[15] Nichols, N.K. Private Communication. University of Reading 2003.

[16] Priestley, A. *A Quasi-Riemann Method for the Solution of One-Dimensional Shallow Water Flow*. Numerical Analysis Report 5/90. University of Reading 1990.

[17] Smith, C.J. *The Semi-Lagrangian Method in Atmospheric Modelling*. Reading University Ph.D. Thesis 2000.

[18] Wilmott, P., Howison, S. and Dewynne, J. *The Mathematics of Financial Derivatives*. Cambridge University Press 1995.

[19] Wilmott, P., Dewynne, J. and Howison, S. *Option Pricing: Mathematical Models and Computation*. Oxford University Press 1993.

[20] Zvan, R., Forsyth, P.A. and Vetzal, K.R. *Discrete Asian Barrier Options*. University of Waterloo, Canada 1998.